The Journal of Experimental Biology 202, 2413–2432 (1999)
Printed in Great Britain © The Company of Biologists Limited 1999
JEB2197

LOCOMOTION IN STURGEON: FUNCTION OF THE PECTORAL FINS

C. D. WILGA* AND G. V. LAUDER

Department of Ecology and Evolutionary Biology, University of California, Irvine, CA 92697, USA

*e-mail: cwilga@uci.edu

Accepted 14 June; published on WWW 25 August 1999

Summary

Pectoral fins are one of the major features of locomotor design in ray-finned fishes and exhibit a well-documented phylogenetic transition from basal to derived clades. In percomorph fishes, the pectoral fins are often used to generate propulsive force *via* oscillatory movements, and pectoral fin propulsion in this relatively derived clade has been analyzed extensively. However, in the plesiomorphic pectoral fin condition, exemplified by sturgeon, pectoral fins extend laterally from the body in a generally horizontal orientation, have been assumed to generate lift to balance lift forces and moments produced by the heterocercal tail, and are not oscillated to generate propulsive force. The proposal that pectoral fins in fishes such as sturgeon generate lift during horizontal locomotion has never been tested experimentally in freely swimming fishes. In this paper, we examine the function of pectoral fins in sturgeon swimming at speeds from 0.5–3.0 $L\,s^{-1}$, where L is total body length. Sturgeon were studied during steady horizontal locomotion as well as while sinking and rising in the water column. Pectoral fin function was quantified using three-dimensional kinematics to measure the orientation of the fin surface, digital particle image velocimetry (DPIV) was used to describe flow in the wake of the fin and to estimate force exerted on the water, and electromyography was used to assess pectoral fin muscle function. Sturgeon (size range 25–32 cm total length) swam horizontally using continuous undulations of the body with a positive body angle that decreased from a mean of 20° at 0.5 $L\,s^{-1}$ to 0° at 3.0 $L\,s^{-1}$. Both the angle of the body and the pectoral fin surface angle changed significantly when sturgeon moved vertically in the water column. Three-dimensional kinematic analysis showed that during steady horizontal swimming the pectoral fins are oriented with a negative angle of attack predicted to generate no significant lift. This result was confirmed by DPIV analysis of the pectoral fin wake, which only revealed fin vortices, and hence force generation, during maneuvering. The orientation of the pectoral fins estimated by a two-dimensional analysis alone is greatly in error and may have contributed to previous suggestions that the pectoral fins are oriented to generate lift. Combined electromyographic and kinematic data showed that the posterior half of the pectoral fin is actively moved as a flap to reorient the head and body to initiate rising and sinking movements. A new force balance for swimming sturgeon is proposed for steady swimming and vertical maneuvering. During steady locomotion, the pectoral fins generate no lift and the positive body angle to the flow is used both to generate lift and to balance moments around the center of mass. To initiate rising or sinking, the posterior portion of the pectoral fins is actively moved ventrally or dorsally, respectively, initiating a starting vortex that, in turn, induces a pitching moment reorienting the body in the flow. Adjustments to body angle initiated by the pectoral fins serve as the primary means by which moments are balanced.

Key words: sturgeon, locomotion, pectoral fin, flow visualization, hydrodynamics, muscle function, *Acipenser transmontanus*.

Introduction

One of the most prominent features in the evolution of ray-finned fishes is the change in pectoral fin position and function. In the plesiomorphic condition, as represented in extant fishes such as sturgeon and fossil taxa such as *Cheirolepis*, the pectoral fins extend laterally from a ventral insertion on the pectoral girdle and are held in a generally horizontal orientation (Gosline, 1971; Moy-Thomas and Miles, 1971; Rosen, 1982; Bemis et al., 1997). This morphology is also characterized by extension of the basal and radial bones of the fin out from the body surface into the fin and by the presence of non-collapsible fin rays. As a result, the pectoral fins are relatively immobile, and a key function has been assumed to be the generation of lift to compensate for the lift and moments generated by the heterocercal tail and negative buoyancy (Affleck, 1950; Alexander, 1965; Gosline, 1971; Thomson, 1976; Blake, 1983; Ferry and Lauder, 1996). Both living ray-finned fishes, such as chondrosteans, lepisoteids and amiids, and outgroup taxa, such as chondrichthyans, display the plesiomorphic condition.

In contrast, most teleost fishes possess a derived condition in which the pectoral fins extend laterally in a more transverse plane and are located in a relatively dorsal position on the side of the body (Rosen, 1982). In these taxa, the basal and radial bones are contained within the body wall, and that portion of the

fin subjected to fluid forces is composed of flexible, collapsible fin rays. As a consequence, many teleost fishes utilize oscillatory motions of their pectoral fins to generate propulsive forces, and a great deal of experimental work (sometimes combined with hydrodynamic theoretical modeling) has been conducted on the function of the pectoral fins in teleost fishes (e.g. Webb, 1973; Blake, 1979, 1981; Geerlink, 1983; Daniel, 1988; Gibb et al., 1994; Drucker and Jensen, 1996, 1997; Lauder and Jayne, 1996; Westneat, 1996; Walker and Westneat, 1997).

In contrast, very little experimental work has been done on locomotion in fishes possessing the plesiomorphic pectoral fin morphology. Despite the use of mechanical models, experiments on dead animals or manipulations of living animals conducted by Daniel (1934), Aleev (1969) and Harris (1936) and the proposed functions of pectoral fins hypothesized on the basis of analyses of the heterocercal caudal fin (Affleck, 1950; Alexander, 1965; Simons, 1970; Thomson, 1976; Videler, 1993; Ferry and Lauder, 1996), virtually no experimental work has been conducted on the function of pectoral fins in freely swimming fishes. As a result, we lack basic data on the kinematics of pectoral fins in plesiomorphic ray-finned fishes, the extent of fin mobility during locomotion and the extent to which muscle activity is used actively to modulate fin function. In particular, the proposal that the pectoral fins in fishes such as sturgeon generate lift during horizontal locomotion has never been tested experimentally *in vivo*.

Our overall goal in this paper is to investigate experimentally the role of the pectoral fins during locomotion in white sturgeon *Acipenser transmontanus*, a negatively buoyant species with pectoral fin location and morphology representative of the plesiomorphic condition for ray-finned fishes. We investigate pectoral fin function both during steady horizontal locomotion and during vertical maneuvering in the water column. Our specific goals were (1) to quantify the position of the body and fins during both steady swimming and changes in vertical position, (2) to use three-dimensional kinematic analysis to quantify the surface orientation and configuration of the pectoral fins, (3) to use a quantitative flow-visualization technique (digital particle image velocimetry, DPIV) to measure experimentally forces exerted by the pectoral fins on the water, and (4) to use electromyography to assess active recruitment of pectoral fin muscles during locomotion.

Materials and methods

Animals

Juvenile white sturgeon *Acipenser transmontanus* (Linnaeus) were obtained from commercial dealers in northern California. Sturgeon were maintained on a diet of sturgeon chow and housed individually in 20 l aquaria at a temperature of 20±2 °C. Experiments were conducted in a calibrated flow tank maintained at an average temperature of 20±1 °C as in previous studies (Jayne and Lauder, 1995a,c; Lauder and Jayne, 1996). The same five individuals averaging 29 cm in total length (L) (range 25–32 cm) were used for all three experimental protocols described below: kinematics, digital particle image velocimetry (DPIV) and electromyography. Additional fresh-frozen specimens were used for dissection and anatomical studies of pectoral fin morphology.

The sturgeon studied in this paper were approximately 2 years old and are of moderate size compared with newly hatched individuals and very large (3 m) sturgeon decades in age. Given the large size variation in sturgeon species, it is possible that the results presented here might differ from those at these size extremes. The sturgeon studied were also negatively buoyant despite the presence of a non-respiratory phystostomous gas bladder.

Kinematics

Sturgeon were video-taped while swimming in a 600 l flow tank with a working area 82 cm long × 28 cm wide × 28 cm high using a NAC HSV500 high-speed video system at 250 fields s^{-1}. One camera was aimed perpendicular to the side of the flow tank to record a lateral view of the swimming sturgeon, while a second camera focused on a front-surface mirror oriented at 45 ° below the working section of the flow tank to record a ventral view. The two cameras were electronically synchronized for all experimental protocols in this paper. The lateral and ventral images were scaled equally using marked grids. Flow speed was controlled by a variable-speed motor. Two camera arrangements were used: a zoomed-out view of the whole body to examine the effects of speed and behavior on body angle, and a zoomed-in view of the head and pectoral fins for detailed studies of pectoral fin conformation (see Fig. 1). Video sequences were digitized using a customized microcomputer video-analysis program.

Six swimming speeds were examined with sturgeon holding position in the flow: 0.5, 1.0, 1.5, 2.0, 2.5 and 3.0 $L\,s^{-1}$ (where L is total body length). These speeds were chosen to investigate whether sturgeon alter their body angle with swimming speed and to represent a wide range over which sturgeon will swim. Each individual was filmed swimming at all six speeds, except for one individual that could not hold position at speeds above 2.0 $L\,s^{-1}$. Five fields per tailbeat sequence were analyzed at each speed for each individual, giving 145 digitized images for the experiments investigating the effects of speed.

Three swimming behaviors, holding position in the water column, rising in the water column and sinking in the water column, were studied as the sturgeon swam in the flow tank at 1.0 $L\,s^{-1}$. Both camera arrangements described above (Fig. 1) were used to investigate whether sturgeon are capable of altering the angle of the pectoral fins and body while changing position in the water column. We define holding position as the sturgeon maintaining a stationary (within 2 % $L\,s^{-1}$ deviation from a fixed frame of reference) horizontal (yaw and roll) and vertical (pitch) position in the water column. Rising and sinking are defined as maintaining a stationary horizontal position in the water column while increasing or decreasing vertical position by an average of 6.1 cm s^{-1} (rise) or 8.7 cm s^{-1} (sink). Video tapes were carefully reviewed in order to choose sequences in which the fish held horizontal position or ascended or descended smoothly in the water column with minimal lateral, upstream/downstream, pitching or rolling motions (again within 2 % $L\,s^{-1}$ deviation

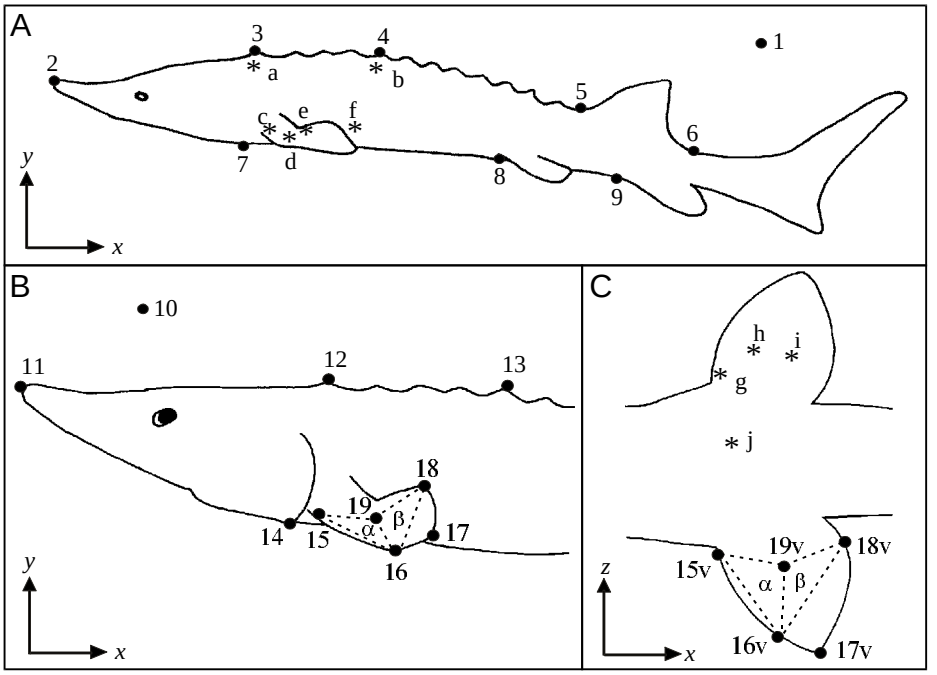

Fig. 1. Schematic diagram of 24 digitized points on the body and pectoral fins of white sturgeon *Acipenser transmontanus*. (A) Lateral view showing the entire body; (B) lateral view of the head and pectoral fin; (C) ventral view of pectoral fin region. Note that the reference axes differ for lateral (*x*, *y*) and ventral (*x*, *z*) views. Data in B and C were gathered simultaneously, while data in A were obtained separately using a different magnification so that the entire animal was visible. Hence, homologous points in A and B are numbered differently. Points 15–18 are the same points in the lateral and ventral views, while points 19 and 19v represent the same location on the dorsal and ventral fin surfaces. These three-dimensional coordinate data were used to calculate a three-dimensional planar angle between the anterior and posterior fin planes (triangles α and β) as shown in B and C. Asterisks and lower case letters indicate the sites of electrode insertion into the pectoral and body musculature, as described in the text (see Materials and methods).

from a fixed frame of reference). However, initiation of rising and sinking sequences by sturgeon necessarily involved pitching movements that resulted from active pectoral fin motion, as described below. The holding, rising and sinking behaviors were chosen *a priori* from video-tape sequences specifically to represent these behaviors to test whether sturgeon are capable of altering their pectoral fin movements with behavior. For all experimental protocols reported in this paper, only sequences in which the dorsal or ventral body surface or the pectoral fins of the sturgeon were at least 4 cm from the sides of the flow tank or surface of the water were analyzed to minimize potential boundary effects from the tank walls on the flow around the fish (Webb, 1993a). Five fields equally spaced throughout each of four tailbeats (mean tailbeat duration is 350 ms) were analyzed for each individual for each behavior, giving 300 digitized images for the whole-body experiments.

The *x* (horizontal) and *y* (vertical) coordinates of nine points on zoomed-out views of the whole body for speed and behavioral analyses were digitized (Fig. 1A): 1, fixed reference mark on the background; 2, snout tip; 3, first dorsal scute tip; 4, fifth dorsal scute tip; 5, anterior base of dorsal fin; 6, dorsal caudal peduncle; 7, ventral gill flap; 8, anterior base of pelvic fin; and 9, anterior base of anal fin.

The *x* and *y* coordinates of ten points on zoomed-in lateral views of the head and pectoral fins were digitized (Fig. 1B): 10, fixed reference mark on the background; 11, snout tip; 12, first dorsal scute tip; 13, fifth dorsal scute tip; 14, ventral gill flap; 15, anterior base of pectoral fin; 16, end of fin spine; 17, lateral fin tip; 18, posterior fin margin; and 19, internal marked location on fin surface. The *x* and *z* coordinates of five points on the pectoral fins in ventral recordings were digitized (Fig. 1C): 15v anterior base of pectoral fin; 16v, end of fin spine; 17v, lateral fin tip; 18v, posterior fin margin; and 19v, medial point on fin.

Prior to filming the zoomed-in views of the head and body, points 15–18 were marked to provide reliable landmarks for subsequent video digitizing. Preliminary recordings without marking the fins revealed that reliable identification of specific points on the fin margins and interior was not possible. Sturgeon were anesthetized using 0.15 g l^{-1} tricaine methanesulfate (MS-222), then intubated and maintained on 0.065 g l^{-1} MS-222 while small aluminum markers were attached to the pectoral fins using cyanoacrylate adhesive. Single larger markers for points 15–18 and 15v–18v were attached such that they wrapped around the edge of the fin and were visible in both lateral and ventral images. Points 19 and 19v consisted of two markers (approximately 0.2 cm×0.2 cm) attached to the dorsal and ventral surfaces of the fin. These interior points were placed at a location where preliminary observations revealed that the posterior region of the fin begins to move dorsally and ventrally during rising and sinking behaviors. Following marker placement, sturgeon were incubated with fresh water until swimming movements commenced, whereupon animals were returned to the flow tank and allowed to recover from anesthesia for at least 3 h prior to video recording.

A three-dimensional planar angle between the two triangles within the pectoral fin (Fig. 1; α and β) (in the animal frame of reference) was calculated, as was the angle made by each of these two triangles with three reference planes in the earth frame of reference. These calculations were used to determine whether the position and conformation of the surface of the pectoral fin are altered among the three behaviors during locomotion. Examination of video recordings and digitized data revealed that motion of the posterior fin region is well

represented by plane β, with nearly all the motion of the entire fin represented by planes α and β together. Inclusion of points 17 and 17v to form additional fin surface triangular elements does not alter the conclusions presented here.

Procedures for these measurements and calculations follow those used in previous research (Ferry and Lauder, 1996; Lauder and Jayne, 1996). Briefly, the working space of the flow tank in which the sturgeon is swimming can be divided into a standard Cartesian coordinate system, and the position of any point in space can be identified by *x*, *y* and *z* values (Fig. 1). The origin of the coordinate system was the lower left corner in the lateral view for the *x* (horizontal) and *y* (vertical) dimensions, and the lower left corner in the ventral view for the *x* (horizontal) and *z* (vertical) dimensions. The *x* coordinate data in the ventral recording were redundant and so were deleted from the analysis, leaving *x*, *y* and *z* coordinates for each point. Triangle α is formed by the *x*, *y* and *z* coordinates of points 15, 15v, 16, 16v, 19 and 19v. Triangle β is formed by the *x*, *y* and *z* coordinates of points 16, 16v, 18, 18v, 19 and 19v. The orientation of the two triangles in three-dimensional space was determined by calculating the angle made with each of three orthogonal reference planes: parasagittal (*xy*), transverse (*yz*) and frontal (*xz*). The parasagittal plane is represented by the side of the flow tank parallel to the swimming sturgeon (visible as the lateral camera view). The transverse plane is equivalent to the front wall of the flow tank towards which the sturgeon is swimming. The frontal plane is represented by the floor of the tank (visible as the ventral view). Since each fin triangle α and β defines a plane, each fin triangle will make a planar angle of intersection with each of the three reference planes. We report these here as external (or earth frame of reference) angles with the *xy*, *yz* and *xz* planes. We also calculated the internal (animal frame of reference) or dorsal angle between planes α and β.

Digital particle image velocimetry

The technique of digital particle image velocimetry (DPIV) was employed to analyze water flow in the wake of the pectoral fins of sturgeon during holding, rising and sinking behaviors (Willert and Gharib, 1991; Lauder et al., 1996; Raffel et al., 1998; Drucker and Lauder, 1999; G. V. Lauder, in preparation). Sturgeon were video-taped swimming at $1.0\,L\,s^{-1}$ using the NAC high-speed video system at 250 fields s^{-1} and the flow tank described above. Fig. 2 illustrates the experimental arrangement used to record water flow patterns. One camera was directed perpendicular to the side of the flow tank to record particle reflections (described below) in lateral (parasagittal) view, while a second camera was aimed at the surface of a mirror positioned at 45° to the side of the flow tank and placed in the flow at a distance of 30–40 cm behind the swimming sturgeon to record a posterior (frontal) view of the position of the sturgeon relative to a laser light sheet. The mirror in the flow tank interfered detectably with water flow only within one mirror width (8 cm) upstream of the mirror, and previous analyses have shown that there is no statistical effect of the presence of such a mirror on locomotor kinematics (Ferry and Lauder, 1996). Water in the flow tank was seeded with near-neutrally buoyant 12 μm diameter silver-coated glass beads that reflected light from a 5 W argon-ion laser focused into a 1–2 mm thick × 10 cm wide light sheet.

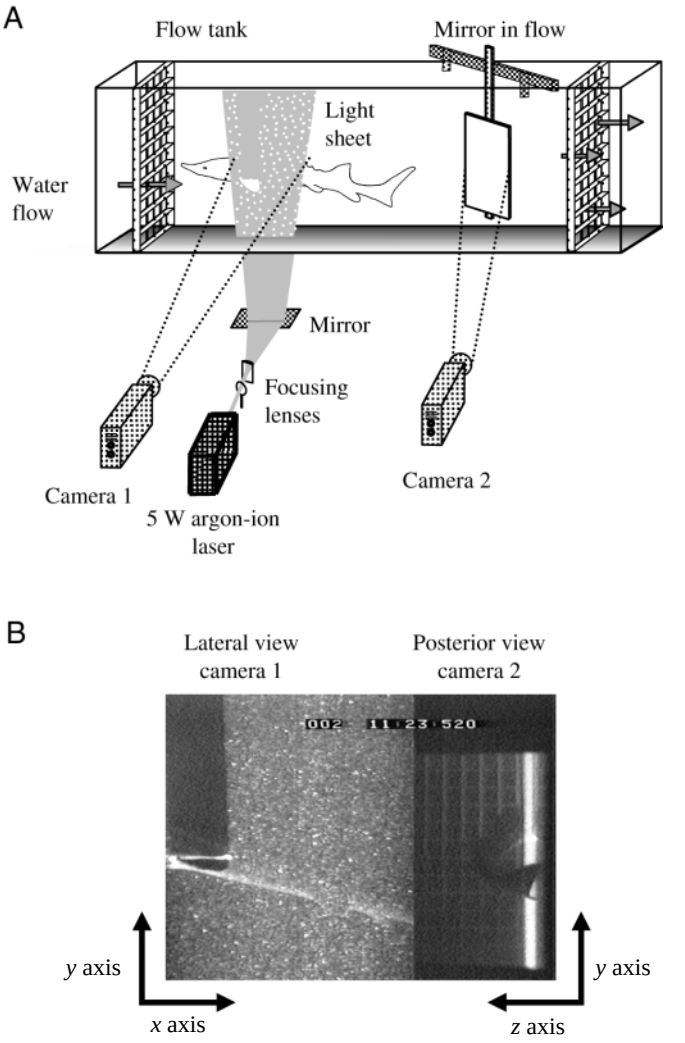

Fig. 2. Schematic diagram of the experimental arrangement used for digital particle image velocimetry (DPIV) data acquisition. (A) The flow tank and the arrangement of the two high-speed video cameras (filming at 250 fields s^{-1}) and the laser. Lenses and mirrors are used to focus the laser beam into a thin (1–2 mm) light sheet that is directed vertically into the flow tank. The sturgeon (considerably exaggerated in size for clarity) is shown with its left pectoral fin cutting through the light sheet. Camera 1 was focused on the particles in the light sheet (shown as white dots) downstream of the pectoral fin to allow quantification of the fin wake. This camera therefore shows a lateral view in the parasagittal plane. Camera 2 views an image reflected from a small mirror (also exaggerated in size for clarity) located in the flow tank downstream of the sturgeon. This camera therefore shows a posterior (transverse) plane which allowed us to visualize how far the pectoral fin extended into the light sheet. The cameras were electronically synchronized, and a split screen provided a composite image of both lateral and posterior views (B). Water flow (indicated by arrows) is from left to right.

Video tapes of particle images during sturgeon locomotion were examined, and sequences in which sturgeon held position

or executed rising or sinking behaviors were identified using the criteria described above for fin kinematics. Sequential pairs of video fields (4 ms apart) of the region of flow just downstream of the pectoral fin were digitized and analyzed by two-frame cross-correlation to yield a 20×20 matrix of 400 velocity vectors according to conventional methods of DPIV analysis (Raffel et al., 1998). Pairs of images were analyzed for three occurrences of each behavior for each individual, giving 27 image pairs analyzed. Where identifiable vortices resulting from fin motion were visible, additional image pairs of the vortex after it moved farther downstream were analyzed to trace the path and strength of the shed vortex.

The pattern of water flow in the wake of the pectoral fin was quantified in three ways. First, plots of the 20×20 matrix of velocity vectors in the wake were examined to reveal flow structure, and the magnitudes and directions of these vectors were calculated to document flow patterns. Flow tank current was subtracted from the matrix of velocity vectors to reveal fluid structures in the wake.

Second, fluid vorticity was calculated from the matrix of velocity vectors to quantify rotational motion in the flow (Vogel, 1994; Krothapalli et al., 1997). To visualize rotational fluid motion, plots of vorticity are presented according to the usual convention (see Figs 9–11) in which a red/orange color indicates counterclockwise fluid movement, a purple/blue color indicates clockwise motion and a greenish color is used to indicate zero vorticity (Krothapalli et al., 1997).

Third, a two-dimensional estimate of the lift force on the pectoral fin was calculated from the matrix of velocity vectors. Lift forces were inferred from the circulation of vortices shed from the trailing edge of the pectoral fin which, according to Kelvin's law, is of equivalent but opposite strength to the bound circulation on the fin (Dickinson, 1996). Circulation (Γ, $cm^2\,s^{-1}$) is a measure of the intensity of a vortex (Vogel, 1994), and the circulation of vortices shed by the pectoral fins was calculated directly from the matrix of velocity vectors using a custom-designed program. In the circulation program, the user defines the circular integration area C around a vortex center interactively against the matrix of velocity vectors. Linear interpolation of the four closest neighboring vectors in the matrix was used to calculate velocities at points on C, and the tangential components around C were summed. Increasing integration of path radii at increments of 0.1 cm was calculated until an asymptotic value for total vortex circulation was detected (Willert and Gharib, 1991). Lift force F (in N) exerted by the pectoral fin on the water was quantified in two dimensions using $F=2m/t$ (Dickinson, 1996), where 2 accounts for the force generated by both fins, m is fluid momentum, and t is the duration of pectoral fin movement digitized from video recordings. Momentum ($kg\,m\,s^{-1}$) was calculated from $m=\rho\Gamma A$, using a density ρ of $1000\,kg\,m^{-3}$, and a cross-sectional area A (cm^2) of the vortex calculated from πr^2, where r is the measured vortex radius.

The lift forces reported in this paper were calculated using data on fluid momentum obtained from a vertical laser light sheet that allows a two-dimensional reconstruction of vortex geometry. Such lift force calculations on the basis of two-dimensional data permit comparative analyses of vortex characteristics and lift forces among behaviors, but do not reflect the total lift force on the fin, for which three-dimensional data are needed (see Drucker and Lauder, 1999; G. V. Lauder, in preparation).

Fin wake vortices were typically observed following movement of the posterior portion of the pectoral fin (plane β). To correlate the velocity of fin motion with relative lift force magnitude and the occurrence of holding, rising and sinking behaviors, the velocity of plane β movement was calculated for the same sequences in which wake vortex force was estimated.

Electromyography

Electromyograms (EMGs) were used to document the sequence of muscle activation relative to pectoral fin movement to determine whether changes in pectoral fin angle are actively controlled by the sturgeon or are the passive result of forces exerted on the fin by fluid motion. Electromyograms, synchronized with high-speed video recordings, were analyzed from four holding, rising and sinking sequences for each of three individuals (26–32 cm total length) swimming steadily at speeds of 1.0 and $2.0\,L\,s^{-1}$. Electromyograms were recorded using bipolar electrodes constructed from 1.8 m lengths of insulated stainless-steel wire 0.051 mm in diameter as in previous research (Jayne and Lauder, 1995b,c; Wilga and Motta, 1998a,b). At the end of each wire, a length of 0.5 mm was stripped of insulation and bent backwards to form a hook. In addition, a third 2 cm long single piece of hooked insulated wire was placed behind each bipolar electrode tip to verify the position of electrode placement in case the electrode was inadvertently pulled out. Sturgeon were anesthetized using $0.15\,g\,l^{-1}$ MS-222, then intubated and maintained on $0.065\,g\,l^{-1}$ MS-222 for the duration of surgery.

Electrodes were implanted using 26 gauge hypodermic needles into 6–9 muscles of the pectoral fin and adjacent body musculature. Dissections prior to implantation provided anatomical landmarks to guide implantation (see Jessen, 1972; Findeis, 1993). The locations of implantations are indicated by asterisks and lower case letters in Fig. 1 (a, epaxialis anterior implant ventral to scute 1; b, epaxialis posterior implant ventral to scute 5; c, dorsal marginal muscle of the pectoral fin; d, fin adductor anterior implant one-third of fin length posterior to the leading edge of the fin; e, fin adductor posterior implant one-third of fin length anterior to the trailing edge of the fin; f, hypaxialis, lateral implant posterior to the trailing edge of the fin; g, ventral marginal muscle of the pectoral fin; h, fin abductor anterior implant one-third of fin length posterior to the leading edge of the fin; i, fin abductor posterior implant one-third of fin length anterior to the trailing edge of the fin). Data from all muscles were recorded simultaneously. Because some electrodes were pulled out during locomotion and some electrodes were not inserted into the target muscle, it was not possible to obtain a complete set of data for all muscles in all individuals.

Following electrode implantation, the electrodes were glued together and tied to a loop of suture in the skin anterior to the fifth dorsal scute. Sturgeon were intubated with fresh water until swimming movements commenced, whereupon animals

were returned to the flow tank and allowed to recover from anesthesia for at least 3 h. At the termination of each experiment, sturgeon were killed with an overdose of MS-222 according to University of California Animal Care and Use Guidelines, and the positions of the electrodes were verified by dissection.

Electrodes were connected to Grass model P511 amplifiers at a gain of 10 000 using high- and low-bandpass filter settings of 100 Hz and 3 kHz, respectively, and a 60 Hz notch filter. Analog EMGs were recorded on a TEAC XR-5000 FM data recorder at a tape speed of 9.5 cm s^{-1}. EMGs and video recordings were synchronized using a pulse generator that provided coded output to both the NAC video system and the TEAC FM tape recorder. The analog EMG signals were converted to digital files using a sampling rate of 8 kHz and filtered using a finite impulse response filter that reduced any signal below 100 Hz to less than 10 % of its original amplitude (Jayne et al., 1990). Digital EMG data were analyzed using a custom-designed computer program to determine the onset and offset times of each EMG burst. In this program, EMG traces were examined visually on a computer monitor, and onset and offset times of each EMG burst were located and digitized and durations calculated.

Statistical tests

Polynomial and linear regression analyses were performed using the following dependent and independent variables and adjusted r^2 values: whole-body angle and flow speed; scute 5 *y* position and proportion of tailbeat; three-dimensional pectoral fin angle and body angle; lift force and fin-flip velocity. For the whole-body and head and pectoral fin variables *versus* behavior analyses, a mixed-model two-way analysis of variance (ANOVA) using Type III sums of squares was performed on the behavior data (Hicks, 1982; SAS Institute, 1996). Behavior was treated as a fixed main effect and individual as a random main effect. Behavior was tested over the behavior × individual interaction term. If a difference was detected by ANOVA, then a Student–Newman–Keuls (SNK) multiple-comparisons test was performed on the data. The data were tested for homogeneous variances using the Levene median test ($P<0.05$) and for normal distribution using the Kolmogorov–Smirnov test ($P<0.05$). Statistical tests were performed using SAS v. 6.12 or SigmaStat v. 2.01 statistical software or calculated using Zar (1996).

Results

Body and pectoral fin kinematics

Sturgeon swimming in the flow tank hold position using continuous undulations of the body and tail and possess a positive body tilt relative to the flow that decreases with increased speed (Fig. 3). At 0.5 *L* s^{-1} body tilt averaged nearly 20 ° and decreased to 0 ° at 3.0 *L* s^{-1}. In this study, *A. transmontanus* exhibited undulatory swimming from 0.5 to

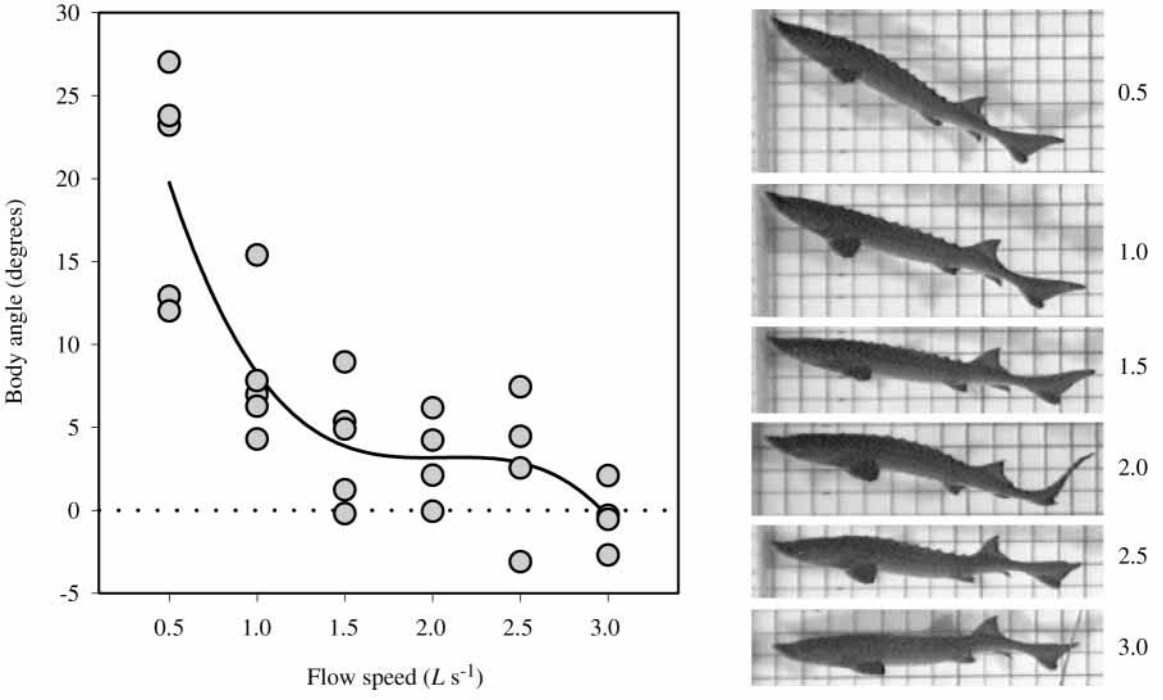

Fig. 3. Graph of body angle *versus* flow speed to show the decreasing angle of the body with increasing speed. Each symbol represents the mean of five body angle measurements (equally spaced in time) during a single tailbeat for each of the five individuals studied. Images on the right show body position at the corresponding to flow speeds in *L* s^{-1}, where *L* is total body length (flow direction is left to right). At all speeds, sturgeon are holding both horizontal and vertical position in the flow, and not rising or sinking in the water column. Points shown as circles, on this and subsequent graphs, indicate that the sturgeon was holding horizontal and vertical position. The curve is a third-order polynomial ($y=41.58–52.27x+27.41x^2–4.44x^3$; adjusted $r^2=0.72$; $P<0.001$), which is a significantly better fit to the data than a second- or first-order equation.

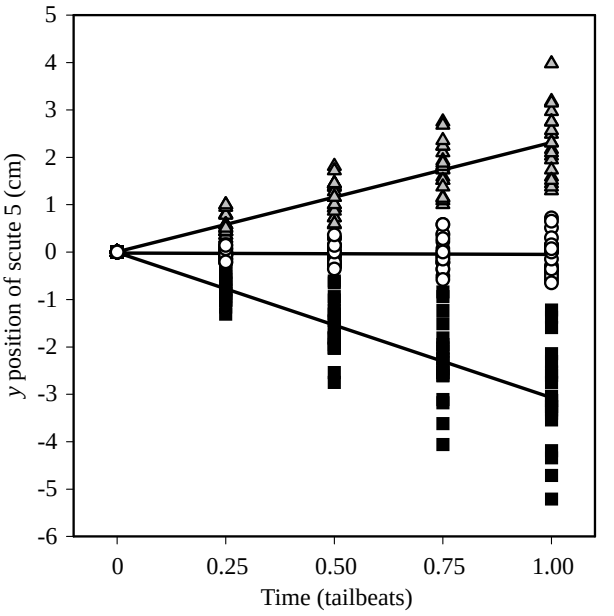

Fig. 4. Graph of the *y* position of scute 5 (points 4 and 13 in Fig. 1) *versus* time (as a proportion of a tailbeat) to show the pattern of body movement during the three behaviors studied. All data are for locomotion at $1.0\,L\,s^{-1}$, where L is total body length. Each point represents one measurement of body position for one individual. Data are shown for five sequences for each of three behaviors, for each of five individuals. Circles indicate holding behavior, triangles show rising behavior, and squares reflect sinking behavior. Data were adjusted to an initial scute position of zero. Least-squares regression lines are shown for each behavior. The slopes are significantly different among the behaviors (P<0.0001), with the slope for holding behavior not significantly different from zero (P=0.67).

$2.0\,L\,s^{-1}$, and the transition to burst-and-glide swimming did not take place until $2.5\,L\,s^{-1}$. Incremental evaluation of the polynomial regression revealed that a third-order polynomial gave a significantly better fit to the data (Fig. 3) than a second- or first-order equation (P=0.034). Sturgeon swam at a significantly higher body angle at $0.5\,L\,s^{-1}$ than at all higher speeds (P<0.001).

Plots of *y* coordinate values of five points digitized along the body (points 2–6 on Fig. 1) confirmed that the sturgeon were swimming horizontally during holding behaviors and smoothly rising and sinking (instead of pitching or yawing) during the rise and sink sequences selected from video recordings of locomotion. In addition, sturgeon did not drift vertically while holding position in the holding sequences analyzed. Fig. 4 shows the *y* position of scute 5 during rising, holding and sinking behaviors at $1.0\,L\,s^{-1}$ during one tailbeat. The data shown are incremental vertical changes from an initial scute position of zero. Comparison of the least-squares linear regressions shows that the slopes are significantly different for each behavior: rise $y=0.0071+2.309x$; hold $y=-0.0162-0.0312x$; sink $y=-0.00740-3.063x$ (P<0.0001). In addition, the slope for holding behavior is not significantly different from zero (P=0.67).

Sturgeon varied the angle of the body relative to the flow while changing position in the water column at $1.0\,L\,s^{-1}$ (Table 1; Fig. 5). A positive body tilt was adopted during rising (mean 19 °), a negative body tilt during sinking (mean −10 °) and a positive body angle while holding position (mean 8 °).

Three-dimensional data on pectoral fin angles show that the conformation of the fin surface changes significantly during the initiation of sinking and rising behavior from an initial holding position at $1.0\,L\,s^{-1}$ (Fig. 6). In contrast, the conformation of the fin during holding does not change throughout the tailbeat cycle. During holding behavior, the pectoral fin is held with a mean dorsal angle of 186 ° between planes α and β (Table 1), which indicates that the fin is held in a slightly concave downwards position; if the internal angle were 180 °, α and β would be coplanar and the fin would be held straight like a rigid flat plate. During rising behaviors, the internal angle increases to an average of 193 °, indicating that the fin is held in an even more concave downward orientation, whereas during sinking behavior the fin becomes concave upwards with a mean internal angle of 170 ° (Table 1). This change in angle reflects the reorientation of the fin to redirect water flow to reposition the body for rising and sinking behaviors. Video recordings show that changes in internal fin angle precede the change in body angle associated with a rise or sink and serve to initiate the pitching moment involved in reorienting the body from the holding position to the more extreme positive body angles associated with rising in the water column and the negative body angles associated with sinking behavior (Fig. 6).

Pectoral fin movement during locomotion is complex and is best represented by illustrating the angle of the two fin planes with respect to each of the three external reference planes.

Table 1. *Summary statistics of kinematic variables in* Acipenser transmontanus *while holding position at 1.0* L *s*$^{-1}$

Variable	Hold	Rise	Sink	*P*-value	SNK
Body tilt angle relative to flow (degrees)	8±1.0	19±1.2	−10±1.2	0.0001*	R>H>S
Pectoral fin angle between α and β triangles (degrees)	186±2.6	193±2.0	170±5.8	0.0991	R,H>S

*Significant at the Bonferroni-corrected ANOVA, *P*-value of 0.01. SNK, Student–Newman–Keul results.
H, hold; R, rise; S, sink.
L, total body length.
Values are means ± S.E.M. (*N*=5).

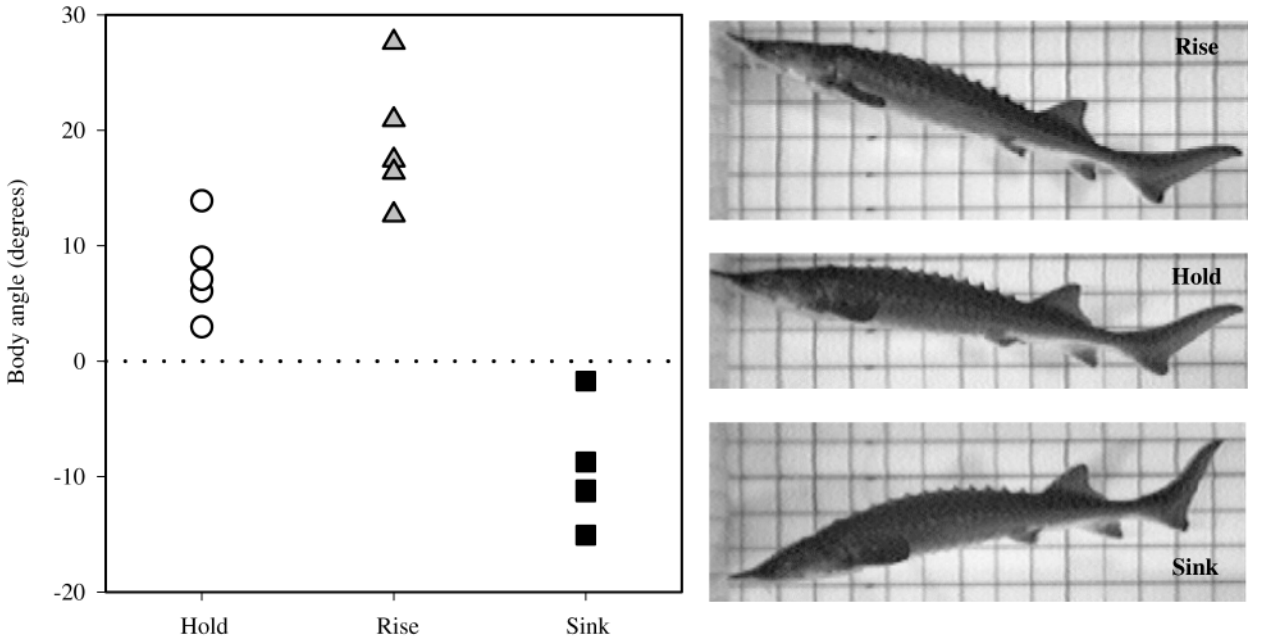

Fig. 5. Comparison of three behaviors *versus* body angle during locomotion at $1.0\,L\,s^{-1}$, where L is total body length. Symbols are as in Fig. 4. Body angle was calculated using the line connecting points 7 and 9 (Fig. 1) and the horizontal (parallel to the flow). Each point represents the mean of five sequences for each of five individuals. Images to the right show a representative body position during rising, holding and sinking behaviors. Body angle is significantly different among the three behaviors (ANOVA, $P<0.0001$).

These data are summarized in Table 2 and depicted graphically in Figs 7 and 8. During holding behavior, sturgeon pectoral fins were held out from the body at 57 ° from the parasagittal (*xy*) plane as measured ventrally; Fig. 7, posterior view, 123 ° as measured dorsally in Table 2), the trailing fin edge is dorsal to the leading edge, and the fin chord is inclined at −11 ° to the flow (Fig. 8). The angle of attack is thus negative during holding behavior, and the most lateral point on the fin is significantly ventral to both the base of the fin and the posterior fin margin.

During sinking behaviors, the fin changes orientation significantly from its configuration during holding position with respect to all three reference planes (Table 2). The posterior portion of the fin tips up relative to the base, the lateral fin edge is more dorsally located relative to the holding position, and the fin chord is oriented at an angle of attack of −29 ° (Figs 7, 8). During rising, the pectoral fin tips so that the trailing edge is ventral to the leading edge, and the fin chord is at a positive 12 ° to the flow.

Digital particle image velocimetry (DPIV)

The structure of water flow in the wake of the pectoral fin during each of the three behaviors was visualized using DPIV. Velocity vectors superimposed on the corresponding video image and the calculated vorticity field are shown for each behavior in Figs 9–11. The left pectoral fin was visible as it extended through the light sheet, and the ventral body margin of the sturgeon was often faintly visible also.

DPIV results of sinking behavior in sturgeon show that a clockwise vortex (negative vorticity) was produced as the pectoral fin flipped upwards to initiate a sinking event (Fig. 9). As documented in the analysis of fin kinematics above, the posterior edge of the fin was angled dorsal to the leading edge during sinking events. In some sinking events, a strong upward flow behind the fin was visualized as upward-pointing vectors,

Table 2. *Summary statistics of three-dimensional planar angles in the pectoral fin of* Acipenser transmontanus *while holding position at 1.0* L s^{-1}

Plane	Triangle	Hold (degrees)	Rise (degrees)	Sink (degrees)	*P*-value	SNK
xz	α	149±4.1	204±6.7	137±2.1	0.0002*	R>H>S
xz	β	182±8.3	207±6.8	153±9.1	0.0002*	R>H>S
yz	α	83±1.4	98±1.7	65±2.3	0.0070*	R>H>S
yz	β	90±1.6	106±1.8	68±3.8	0.0001*	R>H>S
xy	α	123±1.4	124±1.8	116±1.8	0.0060*	R>H,S
xy	β	124±1.3	124±1.8	116±2.0	0.0018*	H,R>S

*Significant at the Bonferroni-corrected ANOVA, *P*-value of 0.008. SNK, Student–Newman–Keul results.

H, hold; R, rise; S, sink.

In the *xz* plane (floor of tank), 0 ° is anterior and 180 ° is posterior, and in the *yz* (anterior side of tank towards which the fish is facing) and *xy* (back side of tank to the right of the fish) planes, 0 ° is dorsal and 180 ° is ventral.

Note that the orientation of the β triangle to the perpendicular of the *yz* plane represents the plane of the posterior portion of the pectoral fin relative to the flow.

Values are means ± S.E.M. (N=5).

L, total body length.

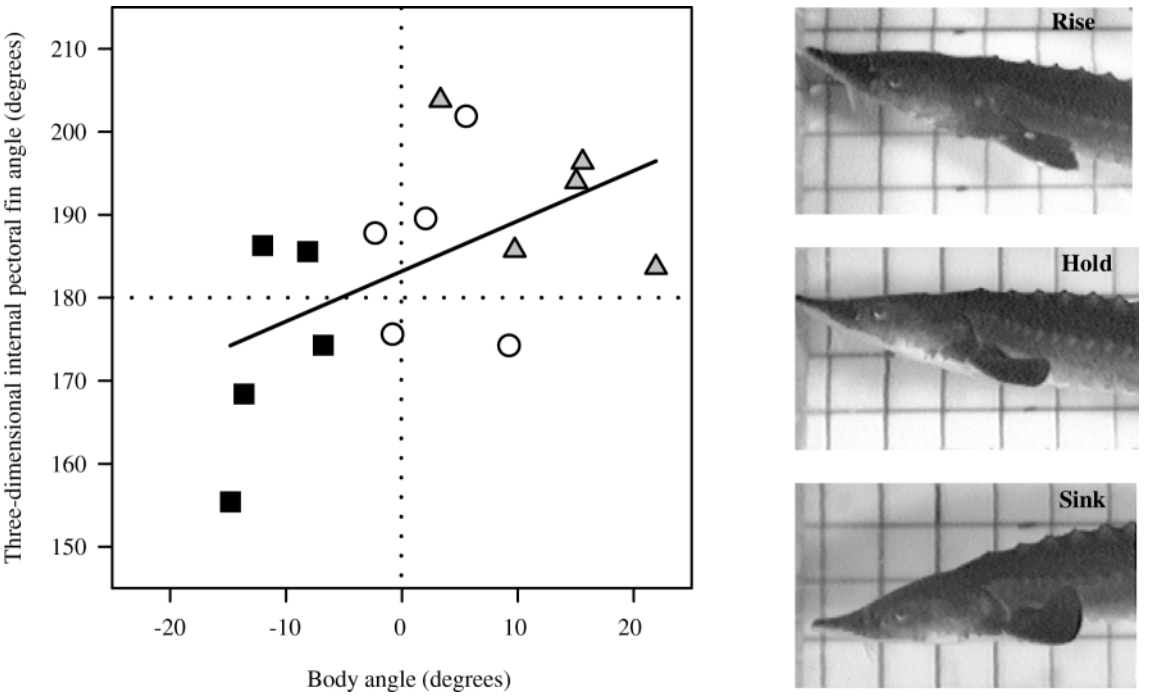

Fig. 6. Graph of internal three-dimensional pectoral fin angle *versus* body angle for each of the three behaviors during locomotion at 1.0 $L\,s^{-1}$, where L is total body length. Symbols are as in Fig. 4. Body angle was calculated using the line connecting points 11 and 13 (see Fig. 1) and the horizontal (parallel to the flow). Each point represents the mean of five sequences for each individual, and data are shown from five individuals. Images to the right show representative head and pectoral fin positions during rising, holding and sinking behaviors. Pectoral fin angles equal to 180° show that the two fin triangles are coplanar; angles less than 180° indicate that the posterior fin margin is concave dorsally; angles greater than 180° indicate that the posterior fin margin is concave ventrally. The least-squares regression line is significant (slope 0.61, $P<0.001$; adjusted $r^2=0.28$).

indicating that a jet of water was being moved upwards from underneath the pectoral fin as seen in Fig. 9. The clockwise vortex is indicated by the blue region of rotating fluid in the vorticity plot. As sturgeon rise, a counterclockwise vortex (Fig. 10; dotted circle on the left and red/yellow center of vorticity on the right) was produced and shed from the fin as it flipped downwards to initiate pitching up of the body. In rising events, flipping of the fin downwards occurs as the posterior edge of the fin moves ventral to the leading edge. Essentially no vorticity was detected by the DPIV analyses of sturgeon while holding position, as indicated by the horizontally oriented vectors and the nearly solid green vorticity field (Fig. 11).

Mean values for circulation, momentum, lift force and fin velocity were calculated from the velocity vector matrix and from video recordings of pectoral fin movement during each of the three behaviors (Table 3). Clockwise vorticity in the wake observed during sinking corresponds to a negative lift force on the pectoral fin that is significantly different from zero (mean lift −0.054 N; $P<0.001$) and acts to pitch the body downwards. Similarly, the counterclockwise vorticity in the wake observed during rising corresponds to a significantly positive lift force on the pectoral fin that acts to pitch the body upwards (mean lift 0.026 N; $P=0.001$). Mean lift force values obtained during position-holding were not significantly

Table 3. *Summary statistics of digital particle image velocimetry variables in* Acipenser transmontanus *while holding position and changing position at 1.0* L s^{-1}

Variable	Hold	Rise	Sink	ANOVA *P*-value
Lift force (N)	−0.00234±0.0024	0.02615±0.0093	−0.05373±0.0093	0.0050*
Fin velocity (m s^{-1})	0.00656±0.0059	−0.06284±0.0054	0.04928±0.0054	0.0001*
Circulation ($m^2\,s^{-1}$)	−0.00040±0.0007	0.00309±0.0007	−0.00592±0.0006	0.0361*
Momentum (kg m s^{-1})	−0.00035±0.0013	0.00294±0.0012	−0.00835±0.0012	0.0211*

*Significant at the Bonferroni-corrected ANOVA, *P*-value of 0.01.
L, total length.
Values are means ± S.E.M. (N=5).

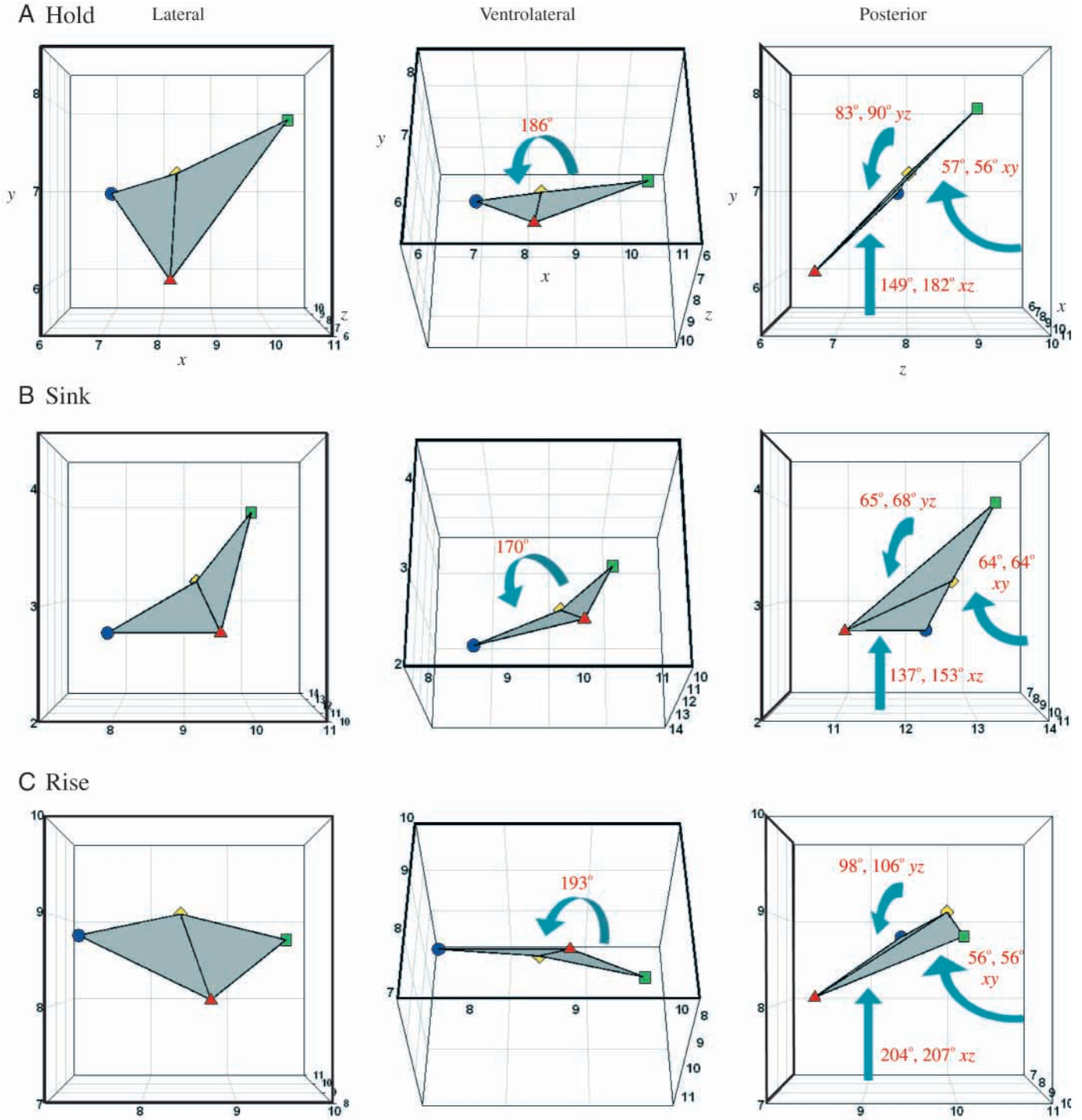

Fig. 7. Orientation of the two pectoral fin planes (α and β) in three-dimensional space during holding, sinking and rising behaviors. The three columns show lateral, ventrolateral and posterior views of the fin triangles, respectively. Points defining the fin triangles correspond to the following digitized locations in Fig. 1: blue circle, point 15; red triangle, point 16; yellow diamond, point 19; green square, point 18. The homologous *xy* plane is outlined in bold in each panel to assist in identifying the rotational view. The internal fin angle between planes α and β is given in the ventrolateral view column, and the angles of each fin triangle are given with respect to the three external reference planes in the posterior view column. The first and second numbers indicate the external three-dimensional angles of the α and β triangles, respectively; note that in the posterior view column the angles are given as acute to the *xy* plane and are therefore the complement to the angles reported in Table 2.

different from zero (Table 3; P=0.340), indicating that the three-dimensional orientation of the pectoral fin during holding is such that no significant lift forces are generated. Similar levels of non-significant vorticity were found in the wake of the pectoral fin at five intervals throughout the tailbeat cycle in several sequences while holding position.

Lift forces generated by the pectoral fin are significantly different among the three behaviors, and the least-squares linear regression of fin-flip velocity *versus* lift force is significant (Fig. 12). Sinking events that have negative lift forces are associated with an upward fin flip (positive velocities by our convention) and are located in the lower right quadrant of Fig. 12. In contrast, rising events that have positive lift forces and are generated by downward fin flips (negative velocities) are located in the upper left quadrant of Fig. 12. Holding events, in which the fin does not flip up or down, cluster around zero lift force and zero fin-flip velocity.

Electromyography

Electromyography of pectoral fin muscles in swimming sturgeon reveals an almost complete absence of muscle activity while holding position at 0.5 and $1.0\,L\,s^{-1}$ (Fig. 13); during holding behavior, the pectoral fins show no discernible movement. In contrast, the abductor muscles in the pectoral fin are active during rising and show strong activity at the initiation of the rise (Fig. 13) when the posterior margin of the pectoral fin moves ventrally to pitch the head up and tilt the body at an increased angle to the flow. During sinking behaviors, the adductor muscles are active, with virtually no activity in the other muscles (Fig. 13); strong adductor activity is seen at the start of sinking when the posterior fin margin flips dorsally, pitching the head ventrally and decreasing the angle of the body to the flow.

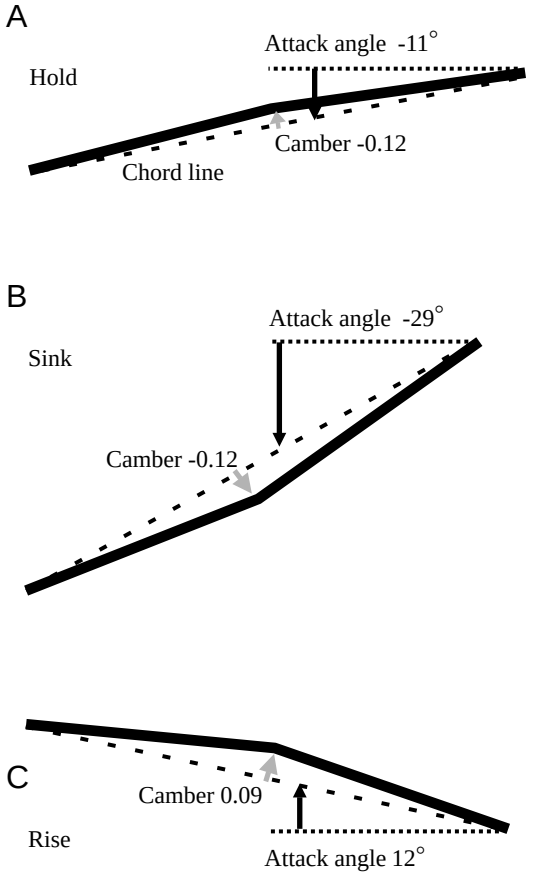

Fig. 8. Schematic diagram of the pectoral fin chord, camber and orientation during holding, sinking and rising behaviors. The pectoral fin is represented as two planes seen edge-on, and camber is calculated as described by Kundu (1990). Note that, during steady horizontal swimming (holding behavior), the pectoral fin has a negative angle of attack and is inclined downwards with respect to the flow, which is parallel to the horizontal dotted line. The angle of attack is given between the chord line and the flow.

There is increased muscle recruitment at higher swimming speeds compared with slower speeds (Fig. 14). During holding behavior at $2.0\,L\,s^{-1}$, the adductors and abductors of the pectoral fin are active alternately to stiffen the fin against increased drag. Abductor muscles are strongly active during rising, while there is little activity in the adductor muscles. The anterior epaxial musculature is also active during rising behavior to raise the head and increase the head angle to the flow, thus contributing to a change in force balance on the body and facilitating upward movement in the water column; relatively little activity is seen in the hypaxial muscles. During sinking behavior, the pectoral fin adductors are strongly active, with correspondingly little activity in the abductor muscles. The hypaxial musculature is active to bend the head ventrally (Fig. 14) and to facilitate downward body pitching to initiate and maintain the sinking posture.

At the end of rise or sink events, antagonistic pectoral fin muscle activity occurs as rising or sinking slows and then stops (the adductors are active as rising stops and the abductors are active as sinking stops). This coincides with the return of the posterior portion of the pectoral fin to its initial holding position. The epaxialis also fires as sinking slows.

Discussion

Body position effects

During steady horizontal swimming, *Acipenser transmontanus* uses continuous undulations of the body and caudal fin with a positive body tilt relative to the flow that decreases with increasing flow speed. Mean body tilt at $0.5\,L\,s^{-1}$ is 20°, which decreases rapidly to 8° at $1.0\,L\,s^{-1}$ and then decreases gradually to 0° at $3.0\,L\,s^{-1}$. Since lift increases with the square of velocity, greater lift is produced at higher flow speeds (Vogel, 1994), and sturgeon appear to be modulating the lift generated by the body profile by altering the angle of attack of the body. Sturgeon are often found in rivers and estuaries (Scott and Crossman, 1973; McGillis, 1984) where they may use lift induced by flow over the body to overcome negative buoyancy. Literature images of steady horizontal locomotion in plesiomorphic clades such as sturgeon frequently depict fish swimming with the ventral body surface oriented in a strictly horizontal plane (e.g. Carter, 1967). However, in the flow tank at speeds less than $2.5\,L\,s^{-1}$, white sturgeon invariably swam with a positive body angle of attack, and this angled posture is critical to the overall force balance during steady swimming and maneuvering discussed below. Dorsal views of swimming sturgeon will not reveal this tilted posture, and changes in body orientation with speed may not be detected with such camera views.

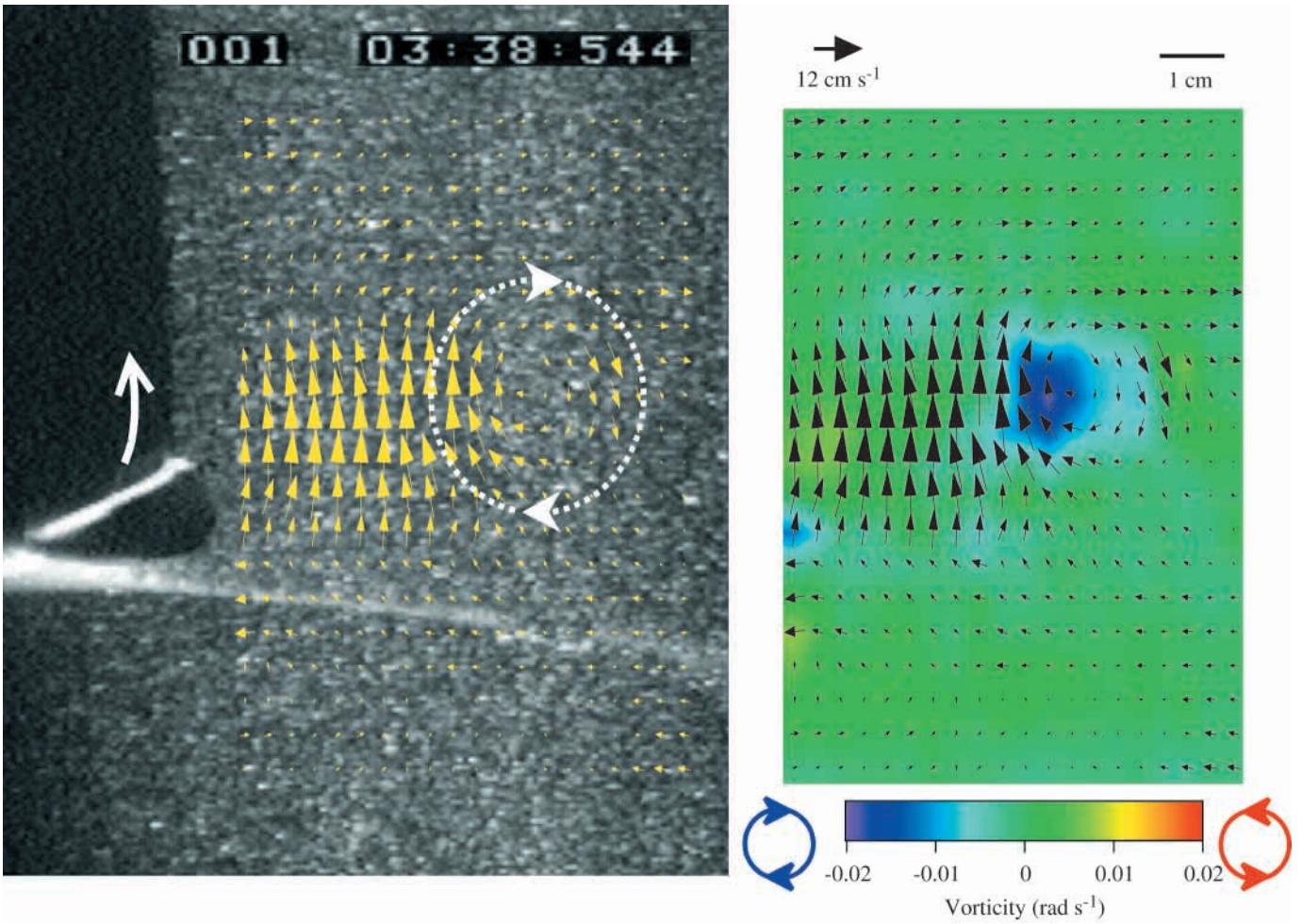

Fig. 9. Digital particle image velocimetry (DPIV) data from sturgeon pectoral fins during sinking behavior. The video image (on the left) shows a single video image of a sturgeon with the left pectoral fin located in the laser light sheet. Note that the posterior edge of the fin is angled dorsal to the leading edge and that the ventral body margin is faintly visible through the light sheet. The 20×20 matrix of yellow vectors downstream of the pectoral fin represents the results of DPIV calculations based on particle images visible as the speckled pattern in the light sheet. The light sheet, which originates below the flow tank, is blocked by the pectoral fin, which casts a dorsal shadow. Note that there is a strong upward flow behind the fin and a clockwise vortex (enclosed by the white dotted circle) which resulted from the upward fin flip (white arrow) to initiate the sinking event. The plot on the right shows fluid vorticity with superimposed velocity vectors (scaled to the same size as the vector matrix in the video image); the clockwise vortex is indicated by the blue region of rotating fluid. Note that a green color indicates no fluid rotation, a blue color reflects clockwise fluid rotation and a red/yellow color indicates counterclockwise fluid rotation. To assist in visualizing the flow pattern, a mean horizontal flow (U) of 29 cm s^{-1} was subtracted from each vector.

Both negatively and neutrally buoyant fishes have been observed to adopt a tilted body attack angle when swimming at low speeds (He and Wardle, 1986; Webb and Weihs, 1994). Tilting in neutrally buoyant fishes has been proposed to be a behavioral mechanism to increase stability control during low-speed swimming when other stabilizers, such as the swimbladder, lose their effectiveness (Webb, 1993b). In addition, tilting in negatively buoyant fishes has been proposed to increase the total area generating lift by using the body as a hydrofoil at low swimming speeds when lift from the pectoral fins is presumably insufficient (He and Wardle, 1986).

The transition from undulatory swimming to burst-and-glide swimming took place at 2.5 $L\,s^{-1}$. These results are similar to the study of Webb (1986), in which undulatory swimming in juvenile *A. transmontanus* (mean L=16 cm) was maintained during steady swimming in a flow tank up to the critical swimming speed of 2.45 $L\,s^{-1}$. Adult *Acipenser fulvescens* (range 120–134 cm total length) swam much more slowly during steady swimming in a still-water tank, averaging 0.1 $L\,s^{-1}$ in the 'slow mode' and 0.25 $L\,s^{-1}$ in the 'fast mode' identified by Long (1995). Sturgeon may swim routinely below the speeds studied in the present study (e.g. Foster and Clugston, 1997) and, at such speeds, they may show differences in body angle and pectoral fin conformation depending on how close they are to the bottom and because of the slow locomotor speed. The experimental conditions used in the present study were designed to be highly controlled and to restrict sturgeon to speeds comparable with those studied in other species. During natural unrestricted locomotion in lakes with relatively still water, sturgeon may exhibit a variety of as

yet undescribed locomotor behaviors with novel hydrodynamic consequences.

Our results also show that white sturgeon altered the angle of body tilt while changing position in the water column at $1.0\,L\,s^{-1}$. A mean body tilt of +19 ° is adopted while rising and a mean body tilt of −10 ° during sinking. As discussed below, we propose that these alterations in body position actively assist in vertical maneuvering by altering the force balance on swimming sturgeon and facilitating rising and sinking as appropriate.

Role of the pectoral fins during locomotion

The pectoral fins of *Acipenser transmontanus* do not produce significant lift during steady horizontal swimming at $1.0\,L\,s^{-1}$ despite the positive body angle relative to the flow, in contrast to previous interpretations of pectoral fin function. We recognize that this conclusion is a significant departure from current views in the literature, but three lines of evidence developed in this paper, three-dimensional kinematic measurements of fin orientation (Figs 7, 8), analyses of the pectoral fin wake (Fig. 11) and electromyograms of motor activity while holding position (Fig. 13), all support the conclusion that the pectoral fins do not generate lift forces during steady horizontal locomotion. The planar surface of the fin is held concave downwards relative to the flow while holding position, indicating that the pectoral fin has camber with a mean dorsal obtuse angle of 186 ° between the two planes of the fin (Fig. 7). In addition, the pectoral fin is held such that the angle of attack between the chord line of the fin and the direction of flow is on average −11 ° during steady

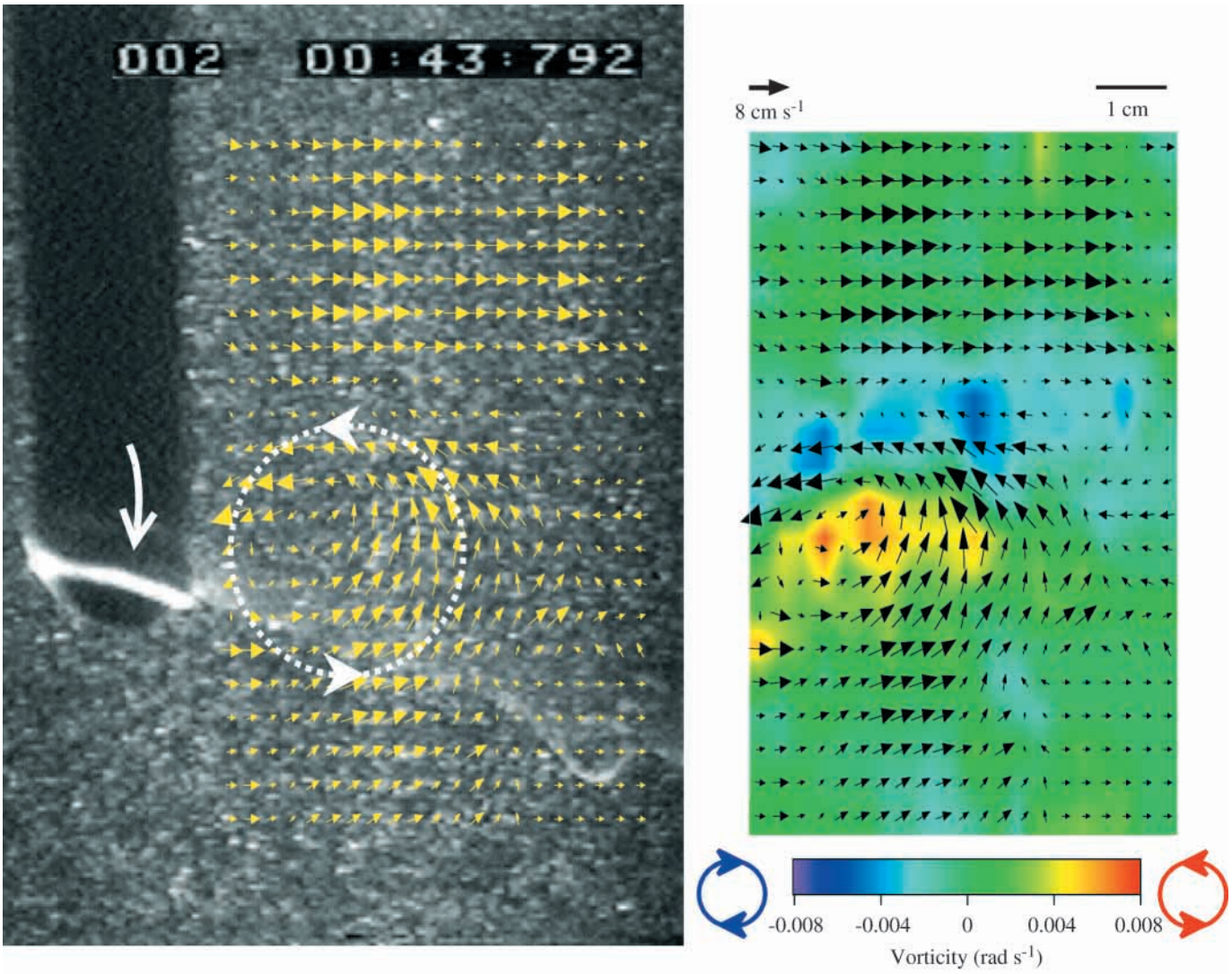

Fig. 10. Digital particle image velocimetry (DPIV) data from sturgeon pectoral fins during rising behavior. Conventions as in Fig. 9. Note that the fin has flipped ventrally (white arrow), with the posterior edge becoming ventral to the leading edge to initiate the rising event, and that a counterclockwise vortex (white dotted circle on the left and orange/red center of vorticity on the right) has been shed from the fin. To assist in visualizing the flow pattern, a mean horizontal flow (U) of $26\,cm\,s^{-1}$ was subtracted from each vector, and vorticity associated with the pelvic fins in the lower right has been deleted.

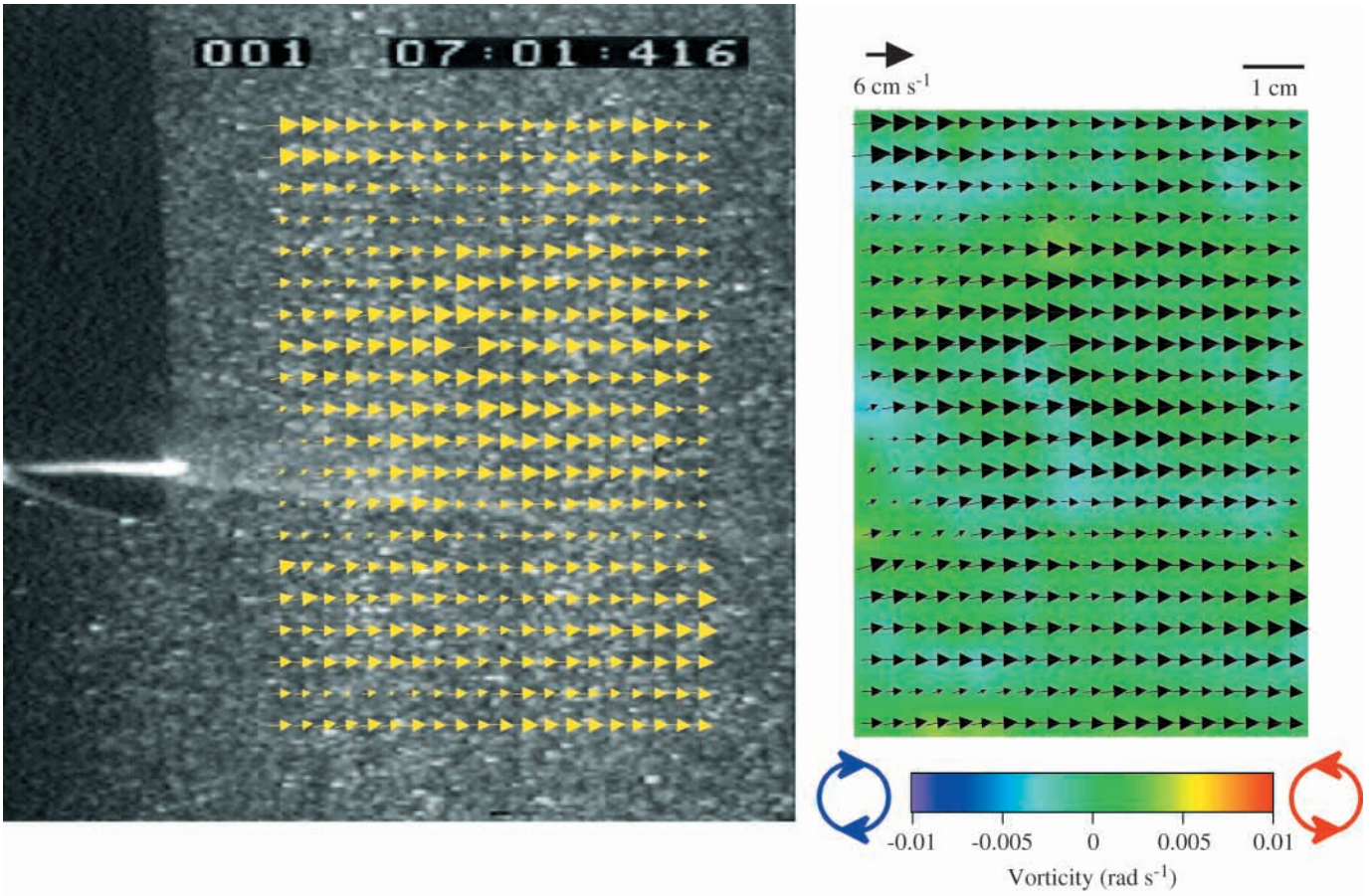

Fig. 11. Digital particle image velocimetry (DPIV) data from sturgeon pectoral fins during holding behavior. Conventions as in Fig. 9. Note that the fin is held in a horizontal position and that the vorticity plot (scaled similarly to Fig. 10) shows effectively no fluid rotation. Hence, the pectoral fins in this position do not generate lift forces. To assist in visualizing the flow pattern, a mean horizontal flow (U) of 24 cm s^{-1} was subtracted from each vector.

horizontal swimming. Therefore, the pectoral fin is being held at an angle of attack relative to the flow that generates no lift or even potentially negative lift, in contrast to the positive lift commonly assumed for pectoral fins of fishes with heterocercal tails (Harris, 1936; Alexander, 1965; Thomson, 1976; Videler, 1993).

The angle of the pectoral fins and body in sturgeon relative to the flow while holding position contrast to position of the wing and fuselage of a cruising airplane. The direction of flow is perpendicular to the *yz* plane and so, according to our conventions, an acute *yz* angle would have a negative angle of attack relative to the flow while an obtuse *yz* angle would have a positive angle of attack (Fig. 7). The anterior and posterior planes of the pectoral fins in the sturgeon make an acute and perpendicular angle respectively to the *yz* plane (Table 2), and thus the anterior plane is at a negative attack angle and the posterior plane is nearly parallel to the flow. Most airplane wings make an obtuse angle to the *yz* plane, and therefore a positive attack angle, relative to the direction of flight while cruising at a constant altitude, which generates positive lift.

Pectoral fins in sturgeon are held at an angle relative to the body that tends to promote maneuvering. The planar surface of the pectoral fins in the sturgeon is held at a negative dihedral angle of –34 ° with respect to the horizontal, or 57 ° between a sagittal section of the body and the *xy* plane. In this position, the fins are destabilizing (Smith, 1992; Simons, 1994) and promote rolling motions of the body, such as those made while maneuvering in the water, rather than preventing rolling as has been suggested (Harris, 1936, 1937). Wings with a positive dihedral angle are oriented such that the planar surface of the wing is tilted dorsally with respect to the horizontal, which resists rolling and restores lateral stability.

Three-dimensional kinematic analyses of the pectoral fins and body of swimming fishes are critical to hypothesizing function accurately. Studies interpreting the pectoral fin of sturgeon and sharks as a two-dimensional rigid flat plate have suggested that the pectoral fins produce lift during steady horizontal swimming (Breder, 1926; Daniel, 1934; Harris, 1936; Aleev, 1969). Indeed, a lateral view of the head and pectoral fin (see Fig. 5; hold) seems to suggest that there is an angle of incidence of approximately 8–10 ° between the flow direction and the anterior margin of the fin (if the fin angle is measured from the anterior base of the pectoral fin to the lateral tip). Quantification of this angle in our animals during steady horizontal swimming also resulted in a positive pectoral fin attack angle of 11 °, similar to the value measured in previous

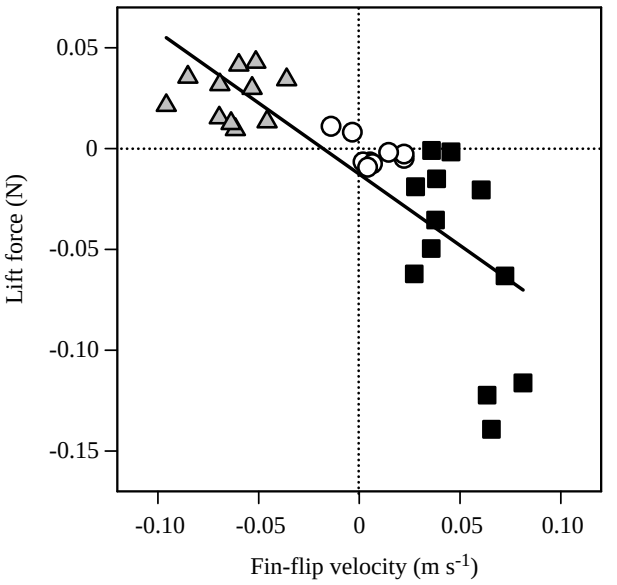

Fig. 12. Graph of the two-dimensional lift force resulting from a pectoral fin flip *versus* pectoral fin-flip velocity. Force was calculated from digital particle image velocimetry (DPIV) measurements (see Materials and methods). Symbols and conventions are as in Fig. 4. Negative velocities are defined as those in which the fin moved ventrally, and negative lift forces are oriented downwards. Note that negative lift forces are associated with an upward fin flip (positive velocities), and that greater force results from higher fin-flip velocities. The least-squares regression line is significant (P<0.001; adjusted r^2=0.60); higher-order regressions were not significant.

studies. However, this two-dimensional angle is extremely misleading as a representation of fin surface orientation. Even though the fin appears to be at a positive angle to the flow in lateral view, three-dimensional kinematics show that the fin is concave downwards with a negative dihedral. The negative-dihedral concave-downwards orientation of the pectoral fin creates a perspective that is very deceiving when viewed laterally, suggesting a positive fin angle of attack when in fact this angle is negative. These errors are similar to those found previously by Lauder and Jayne (1996) and Gibb et al. (1994), who compared two-dimensional views with three-dimensional orientations in studies of pectoral fin kinematics in sunfishes (*Lepomis macrochirus*).

Additional data supporting the conclusion that the pectoral fins of white sturgeon do not produce lift during steady swimming come from the results of our DPIV analyses of the pectoral fin wake. These data show that the pectoral fins are generating no lift while the sturgeon swim horizontally. There was negligible vorticity evident in the wake of the pectoral fins during steady horizontal swimming and, according to Kelvin's law, shed wake vortices must be equivalent in magnitude but opposite in direction to the bound circulation around the pectoral fin (Kundu, 1990; Dickinson, 1996). Thus, the circulation of the shed vortex can be used to calculate the force on the pectoral fin. We calculated the lift force in one plane only, not total lift, allowing us to make a relative comparison between the three behaviors. Mean lift force calculated in the wake of the fins during holding was −0.00234±0.0024 N (mean ± S.E.M.), which is not significantly different from zero (Table 3). This lack of vorticity indicates that, during holding

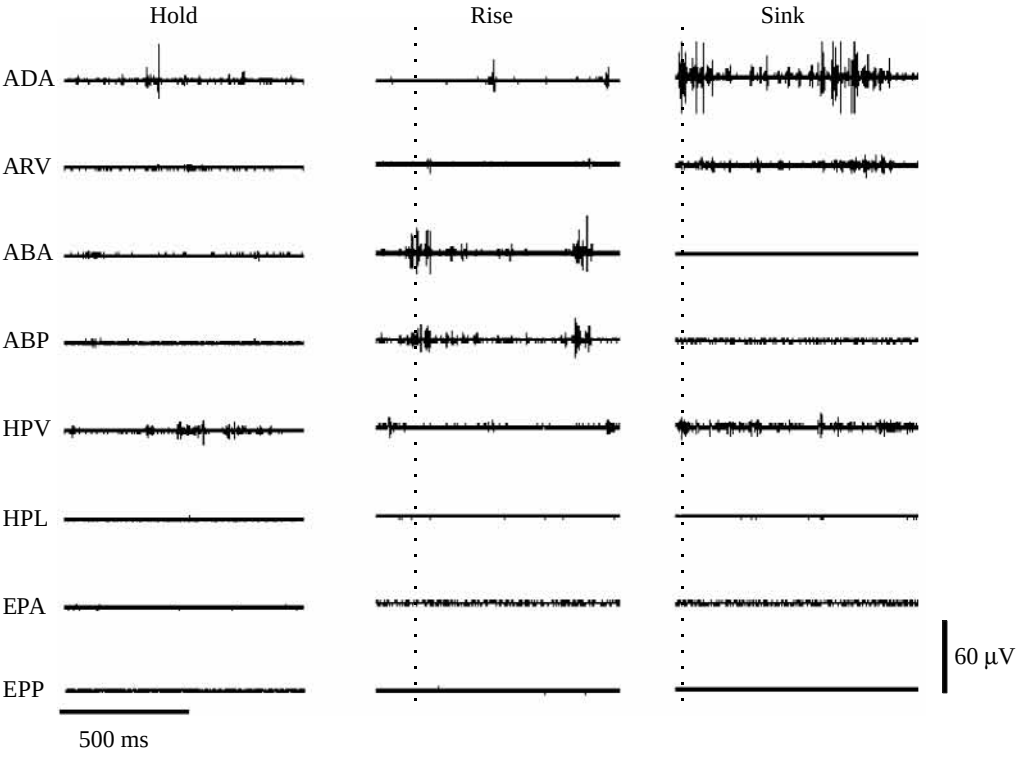

Fig. 13. Electromyographic data from selected pectoral fin and body muscles during locomotion at 1.0 L s^{-1}, where L is total body length, for each of the three behaviors. Vertical dotted lines indicate the initiation of the pectoral fin flip prior to the start of rising and sinking behaviors as determined by an analysis of simultaneously obtained video recordings. Note the near absence of fin muscle activity while holding position. All three panels are from the same individual. ABA, abductor profundus, anterior implant; ABP, abductor profundus, posterior implant; ADA, adductor profundus, anterior implant; ARV, arrector ventralis; EPA, epaxialis, anterior implant; EPP, epaxialis, posterior implant; HPL, hypaxialis, lateral implant; HPV, hypaxialis, ventral implant.

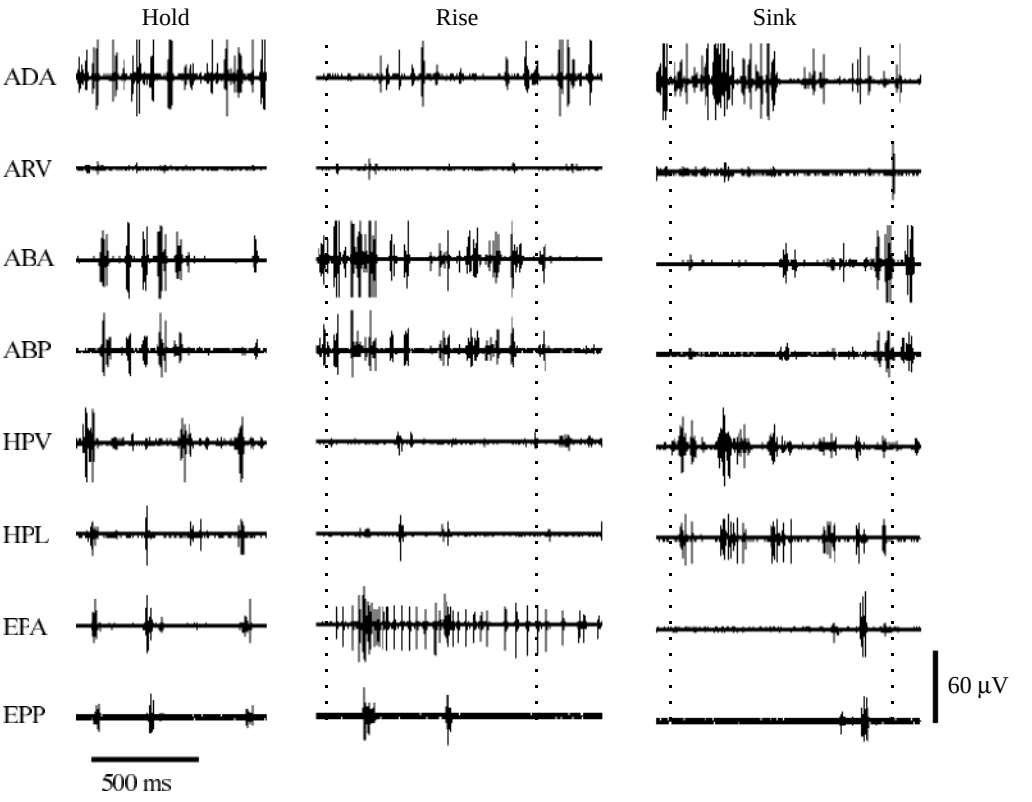

Fig. 14. Electromyographic data from selected pectoral fin and body muscles during locomotion at $2.0\,L\,s^{-1}$, where L is total body length, for each of the three behaviors. The first dotted line in the rising and sinking panels indicates the start of the fin flip, while the second dotted line indicates the end of the fin flip. The timing of both events was determined from an analysis of simultaneous high-speed video recordings of fin movement. Note the increased muscle recruitment compared with locomotion at $1.0\,L\,s^{-1}$ (see Fig. 13). Abbreviations are as in Fig. 13.

behavior, the pectoral fins are oriented in such a way that the pressure and, therefore, the flow speed over and under the wing are equivalent and no lift is generated. Differential pressure between the upper and lower surfaces of the pectoral fin would produce a vortex sheet that is shed from the tips of the fin and rolls up to form a wing-tip vortex (Kundu, 1990). Given the orientation of the light sheet used to image flow (Fig. 2), we were not able to image wing-tip vortices during any locomotor behaviors. However, we predict that such vortices will only be present when sturgeon alter body pitch and maneuver vertically or horizontally in the water, and not during steady horizontal swimming given the orientation of the pectoral fins.

In contrast to horizontal swimming, the pectoral fins of sturgeon actively assist changes in vertical body position by generating negative and positive lift forces during vertical maneuvering. Sinking behavior is initiated when the posterior plane of the fin flips upwards relative to the anterior plane to produce a mean acute dorsal angle of 170° (Table 1). This mechanism is similar to raising the ailerons or spoilers of an airplane wing to slow the speed of the plane for landing (Smith, 1992; Wegener, 1997). At the same time, the leading edge of the fin is rotated downwards relative to the flow such that the chord line is now located above the plane of the fin with an angle of attack of −29° (Fig. 8B). As the posterior plane of the fin flips up, a clockwise vortex is produced and shed from the trailing edge of the pectoral fin, and this vortex is visible in the wake (Fig. 9) and is readily observed using DPIV as it rolls off the fin and is carried downstream.

The opposite wake flow pattern occurs when sturgeon initiate a rising maneuver in the water column. At the beginning of a rise, the posterior plane of the fin flips downwards to produce a mean obtuse dorsal internal fin angle of 193° (Table 1), while the leading edge of the fin is rotated upwards relative to the flow. This flipping down of the posterior portion of the pectoral fin changes the angle of attack to +12° (Fig. 8C) and resembles the lowering of the flaps of an airplane to increase lift during take-off. A counterclockwise vortex is expected in the wake as the result of a ventral fin flip, and such shed vorticity is indeed visualized (Fig. 10).

The lift produced by changes in orientation of the pectoral fin surface during sinking and rising appears to be a mechanism to alter the position of the head and anterior portion of the body. A change in head orientation will alter the force balance on the body as a result of interaction with oncoming flow, and will cause a vertical force that will tend to move the sturgeon ventrally or dorsally. The forces produced by the pectoral fins during sinking are significantly greater in magnitude than those observed during rising. This may be due to the necessity of reorienting the body through a greater angular change to effect sinking, since a positive body tilt is adopted while holding position. To change position from holding to sinking, sturgeon must reposition the body from a positive angle of 8° (mean hold body tilt), through the horizontal to a negative body tilt of −10° (mean sinking body attack), a total of 18°. In contrast, a change in position from holding behavior to rising simply requires that the sturgeon increase the positive tilt of the body by 11° (mean hold minus rise difference), necessitating less total force.

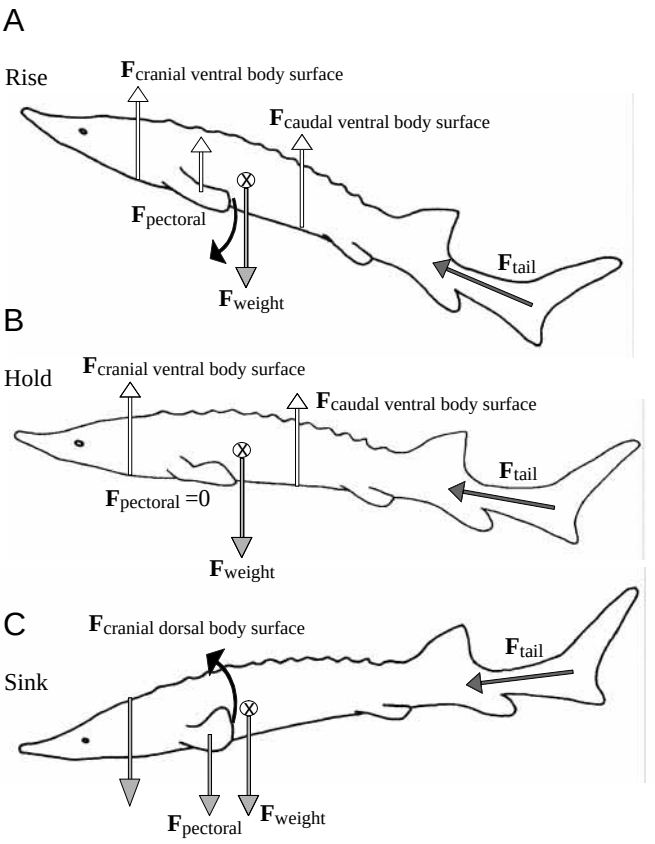

Fig. 15. Diagram of proposed vertical force balance on a swimming sturgeon at $1.0\,L\,s^{-1}$, where L is total body length. X indicates the location of the center of mass, and vectors indicate forces exerted by the fish on the fluid. In all panels, the tail vector is assumed to generate force passing near the center of mass (see text for discussion). Lift forces are generated by the ventral body surface, both anterior and posterior to the center of mass. (A) Rising; (B) holding position (based on the experimental results of this paper, no forces are generated by the pectoral fins during holding); (C) sinking. Curved arrows indicate the fin flip initiating rising or sinking behavior.

Aleev (1969) described experiments in which the pectoral fins in three species of sturgeon were amputated, and he indicated that these fishes were unable to move in midwater and descended to the bottom, where they remained. Although the results of such radical manipulations are difficult to assess because of the wide range of possible reactions to surgery and compensatory factors, it is possible that the absence of the fins prevented the sturgeon from initiating pitch changes using the mechanisms discussed above and therefore from rising off the substratum.

Recruitment of motor activity

Movement of the posterior plane of the pectoral fin during sinking and rising is actively controlled by *Acipenser transmontanus*. At the beginning of a rise, the pectoral fin abductors (ventral fin muscles) are active to depress the posterior third of the pectoral fin (Fig. 1, plane β; Fig. 13) which produces a strong wake vortex (Fig. 10). In contrast, the pectoral fin adductors (dorsal fin muscles) are active during elevation of fin plane β at the beginning of sinking (Fig. 13), also producing a strong wake (Fig. 9). Occasionally, low levels of activity in the arrector ventralis and ventral hypaxial muscles are present during sinking. Virtually no motor activity is present in the pectoral fin muscles, and very little activity in the body muscles while holding position at $0.5\,L\,s^{-1}$ and $1.0\,L\,s^{-1}$, indicating that the pectoral fin is not actively held in its horizontal holding position during steady horizontal locomotion. Pectoral fin muscles are recruited at higher swimming speeds ($2.0\,L\,s^{-1}$) in the sturgeon (Fig. 14), as is the epaxial and hypaxial musculature, which is virtually silent at $1.0\,L\,s^{-1}$. This pattern of effectively no muscle activity at slower speeds and then recruitment at higher speeds differs from the activity patterns recorded in homologous pectoral fin muscles of percomorph teleost fishes using oscillatory fin motions to generate propulsive force (Drucker and Jensen, 1997; Westneat and Walker, 1997). In these species, both adductor and abductor musculature are active at all speeds, although details of activity patterns change as speed increases. Indeed, the pattern of pectoral muscle activation seen in white sturgeon is more similar to the recruitment of red and white axial musculature in fishes as speed increases (Bone, 1978; Johnston, 1981; Rome et al., 1993) where, at threshold speeds, previously inactive muscles are recruited to increase locomotor power. This suggests that a fundamental change in pectoral fin motor activity patterns has taken place during the evolution of ray-finned fish and that the origin of a mobile fin was accompanied by significant alterations in the recruitment threshold for fin adductor and abductor muscles.

At a speed of $2.0\,L\,s^{-1}$, both epaxial and hypaxial muscles become active while holding position, and fin abductor and adductor muscles are alternately active, probably functioning to make small postural adjustments or to stiffen the fin in the faster flow. Approximately four cycles of alternating activity in the pectoral fin muscles occur during an average tailbeat, with no observable change in pectoral fin conformation. Thus, it is unlikely that this alternating muscular activity is evidence that lift is being generated at higher speeds and suggests that pectoral fin muscle activity is used to maintain fin posture. Epaxial and hypaxial muscles are also recruited to elevate or depress the head and anterior body during rising or sinking, respectively, at $2.0\,L\,s^{-1}$. At the initiation of rising behavior at $2.0\,L\,s^{-1}$, during which the head pitches up, nearly constant activity is observed in the cranial region of the epaxialis, while it is virtually silent during holding and sinking. Increased activity in both the ventral and lateral hypaxialis regions takes place during the initiation of sinking behavior compared with activity levels seen during holding and rising behavior. This indicates that the head is actively elevated or depressed during rising or sinking at faster flow speeds and that conformational changes in the anterior body assist forces generated by the pectoral fins to accomplish pitching movement. Antagonistic pectoral fin muscles become active as rising or sinking in the sturgeon slows to a stop (i.e.

the adductors are active as rising stops and the abductors are active as sinking stops), and this activity probably functions to return the conformation of the pectoral fin back to the holding position.

Proposed force balance on swimming sturgeon

The results presented above on sturgeon pectoral fins contrast with previous models of locomotion in fishes such as sturgeon and sharks with heterocercal tails. The classical view holds that the pectoral fins function to generate lift that balances the lift and moments produced by the heterocercal tail (Aleev, 1969; Thomson, 1976; Videler, 1993). According to this classical model, as the heterocercal tail beats, it generates a lift force that is directed dorsally and anteriorly and should deflect water ventrally and posteriorly (Affleck, 1950; Alexander, 1965; Simons, 1970; Ferry and Lauder, 1996). This lift force then produces a turning moment around the center of balance that tends to pitch the head ventrally. The turning moment is thought to be countered by the passage of the upwardly inclined pectoral fins and ventral surface of the head through the water, generating a counteracting lift force that is directed dorsally. Finally, the net upward lift forces are balanced by the weight of the fish and, as a result, the fish continues to swim in a horizontal cruising plane with both vertical forces and moments in balance.

We suggest a new hypothesis for the vertical force balance on sturgeon during steady horizontal swimming and vertical maneuvering in the water column (Fig. 15). The new hypothesis is based on our findings that the pectoral fins generate negligible lift force, and includes the results of Schmidt and Lauder (1995) and G. V. Lauder (in preparation), which show that the heterocercal tail of *A. transmontanus* generates thrust directed near the center of mass of the sturgeon. In our revised hypothesis, four vertical components of force act on the sturgeon during steady horizontal swimming: a downward force at the center of mass, $\mathbf{F}_{\text{weight}}$, due to the negative buoyancy of these fish; an upward force due to the dorsally pitched ventral surface of the body cranial to and caudal to the center of mass, $\mathbf{F}_{\text{cranial ventral body surface}}$ and $\mathbf{F}_{\text{caudal ventral body surface}}$, respectively; and a longitudinal force resulting from caudal fin oscillation, $\mathbf{F}_{\text{tail}}$. The pectoral fins do not contribute significant lift during steady horizontal swimming on the basis of the results presented in this paper. Note that during horizontal locomotion, as shown in Fig. 15B, the body is tilted at a positive angle of attack to the flow (8 ° at $1.0\,L\,s^{-1}$). This new force balance hypothesis during holding behavior suggests that sturgeon adjust their body tilt to balance the forces on the ventral body surface anterior and posterior to the center of mass. Previous proposed force balances have not included the effect of the ventral body surface located posterior to the center of mass, which will also generate a moment.

During vertical maneuvering, the pectoral fins of sturgeon do generate force, and the proposed effects of these forces are illustrated in Fig. 15A,C. Rotation of plane β of the pectoral fins dorsally at the initiation of the sinking event produces a downward force, which causes the anterior region of the body to pitch ventrally. Thereafter, downward movement of the body during the remainder of the sinking event is assisted by the negative pitch of the body interacting with the oncoming flow. Similarly, the rotation of plane β of the pectoral fins ventrally at the initiation of a rising event produces a dorsally directed force, which causes the anterior region of the body to pitch dorsally. Again, dorsal movement of the body during the remainder of the rising event is probably effected by the positive pitch of the body interacting with the oncoming flow. Thus, the pectoral fins in sturgeon appear to be crucial for initiating maneuvering movements in the water column, but not for lift generation during steady horizontal swimming.

Do other clades, such as chondrichthyans, which possess a plesiomorphic pectoral fin morphology, use their pectoral fins to generate lift during horizontal locomotion as predicted by the classical model? Or do such pectoral fins function primarily during maneuvering in a manner similar to that in white sturgeon? In contrast to sturgeon, the heterocercal tail of sharks appears to produce significant lift force (Ferry and Lauder, 1996). However, the function of pectoral fins in sharks has yet to be analyzed experimentally, and such analyses are the next logical step towards understanding the evolutionary transformation of pectoral fin function in fishes.

The authors gratefully acknowledge Eliot Drucker, Alice Gibb, Lara Ferry-Graham, Ted Stankowich, Kate Lauder, Christian Pham and Gary Gillis for providing assistance during the experiments and/or analysis. Stephen Anderson kindly wrote the computer program used to calculate circulation, and Ted Castro-Santos kindly supplied several references. We also thank Eliot Drucker, Alice Gibb, Lara Ferry-Graham, Gary Gillis, Jimmy Liao, Frank Fish, Jen Nauen and Mark Westneat for providing helpful comments or discussion during the course of this project. Support was provided by NSF grants to C.D.W. (DBI 97-07846) and G.V.L. (IBN 98-07012).

References

Affleck, R. J. (1950). Some points in the function, development and evolution of the tail in fishes. *Proc. Zool. Soc. Lond.* **120**, 349–368.

Aleev, Y. G. (1969). *Function and Gross Morphology in Fish* (translated from the Russian by M. Raveh). Jerusalem: Keter Press.

Alexander, R. McN. (1965). The lift produced by the heterocercal tails of Selachii. *J. Exp. Biol.* **43**, 131–138.

Bemis, W. E., Findeis, E. K. and Grande, L. (1997). An overview of Acipenseriformes. *Env. Biol. Fish.* **48**, 25–71.

Blake, R. W. (1979). The mechanics of labriform locomotion. I. Labriform locomotion in the angelfish (*Pterophyllum eimekei*): an analysis of the power stroke. *J. Exp. Biol.* **82**, 255–271.

Blake, R. W. (1981). Influence of pectoral fin shape on thrust and drag in labriform locomotion. *J. Zool., Lond.* **194**, 53–66.

Blake, R. W. (1983). *Fish Locomotion*. Cambridge: Cambridge University Press.

Bone, Q. (1978). Locomotor muscle. In *Fish Physiology*, vol. VII,

Locomotion (ed. W. S. Hoar and D. J. Randall), pp. 361–424. New York: Academic Press.

Breder, C. M. (1926). The locomotion of fishes. *Zoologica* **4**, 159–256.

Carter, G. S. (1967). *Structure and Habit in Vertebrate Evolution*. Seattle: University of Washington Press.

Daniel, J. F. (1934). *The Elasmobranch Fishes*. Berkeley: University of California Press.

Daniel, T. L. (1988). Forward flapping flight from flexible fins. *Can. J. Zool.* **66**, 630–638.

Dickinson, M. H. (1996). Unsteady mechanisms of force generation in aquatic and aerial locomotion. *Am. Zool.* **36**, 537–554.

Drucker, E. and Jensen, J. (1996). Pectoral fin locomotion in the striped surfperch. I. Kinematic effects of swimming speed and body size. *J. Exp. Biol.* **199**, 2235–2242.

Drucker, E. G. and Jensen, J. S. (1997). Kinematic and electromyographic analysis of steady pectoral fin swimming in the surfperches. *J. Exp. Biol.* **200**, 1709–1723.

Drucker, E. G. and Lauder, G. V. (1999). Locomotor forces on a swimming fish: three-dimensional vortex wake dynamics quantifed using digital particle image velocimatry. *J. Exp. Biol.* **202**, 2393–2412.

Ferry, L. A. and Lauder, G. V. (1996). Heterocercal tail function in leopard sharks: a three-dimensional kinematic analysis of two models. *J. Exp. Biol.* **199**, 2253–2268.

Findeis, E. K. (1993). Skeletal anatomy of the North American shovelnose sturgeon *Scaphirhynchus platorhynchus* (Rafinesque 1820) with comparisons to other Acipenseriformes. PhD thesis, Amherst, University of Massachusetts. 444pp.

Foster, A. M. and Clugston, J. P. (1997). Seasonal migration of gulf sturgeon in the Suwannee river. *Trans. Am. Fish. Soc.* **126**, 302–308.

Geerlink, P. J. (1983). Pectoral fin kinematics of *Coris formosa* (Teleostei, Labridae). *Neth. J. Zool.* **33**, 515–531.

Gibb, A., Jayne, B. C. and Lauder, G. V. (1994). Kinematics of pectoral fin locomotion in the bluegill sunfish *Lepomis macrochirus*. *J. Exp. Biol.* **189**, 133–161.

Gosline, W. A. (1971). *Functional Morphology and Classification of Teleostean Fishes*. Honolulu: University of Hawaii Press.

Harris, J. E. (1936). The role of the fins in the equilibrium of the swimming fish. I. Wind tunnel tests on a model of *Mustelus canis* (Mitchell). *J. Exp. Biol.* **13**, 476–493.

Harris, J. E. (1937). The mechanical significance of the position and movements of the paired fins in the Teleostei. *Pap. Tortugas Lab.* **31**, 173–189.

He, P. and Wardle, C. S. (1986). Tilting behavior of the Atlantic mackerel, *Scomber scombrus*, at low swimming speeds. *J. Fish Biol.* **29**, 223–232.

Hicks, C. R. (1982). *Fundamental Concepts in the Design of Experiments*. Orlando: Harcourt Brace Jovanovich College Publishers.

Jayne, B. C. and Lauder, G. V. (1995a). Speed effects on midline kinematics during steady undulatory swimming of largemouth bass, *Micropterus salmoides*. *J. Exp. Biol.* **198**, 585–602.

Jayne, B. C. and Lauder, G. V. (1995b). Red muscle motor patterns during steady swimming in largemouth bass: effects of speed and correlations with axial kinematics. *J. Exp. Biol.* **198**, 1575–1587.

Jayne, B. C. and Lauder, G. V. (1995c). Are muscle fibers within fish myotomes activated synchronously? Patterns of recruitment within deep myomeric musculature during swimming in largemouth bass. *J. Exp. Biol.* **198**, 805–815.

Jayne, B. C., Lauder, G. V., Reilly, S. M. and Wainwright, P. C. (1990). The effect of sampling rate on the analysis of digital electromyograms from vertebrate muscle. *J. Exp. Biol.* **154**, 557–565.

Jessen, H. (1972). Schultergurtel und Pectoralflosse bei Actinopterygiern. *Fossils & Strata* **1**, 1–101.

Johnston, I. A. (1981). Structure and function in fish muscle. *Symp. Zool. Soc. Lond.* **84**, 71–113.

Krothapalli, A., Lourenco, L. and Shih, C. (1997). Visualization of velocity and vorticity fields. In *Atlas of Visualization III* (ed. Y. Nakayama and Y. Tanida), pp. 69–82. Boca Raton: CRC Press.

Kundu, P. (1990). *Fluid Mechanics*. San Diego: Academic Press.

Lauder, G. V., Connon, C. and Dunn-Rankin, D. (1996). Visualization of flow behind the tail of swimming fish: new data using DPIV techniques. *Am. Zool.* **36**, 7A.

Lauder, G. V. and Jayne, B. C. (1996). Pectoral fin locomotion in fishes: testing drag-based models using three-dimensional kinematics. *Am. Zool.* **36**, 567–581.

Long, J. H. (1995). Morphology, mechanics and locomotion: the relation between the notochord and swimming motions in sturgeon. *Env. Biol. Fish.* **44**, 199–211.

McGillis, S. M. (1984). *Freshwater Fishes of California*. Berkeley: University of California Press.

Moy-Thomas, J. A. and Miles, R. S. (1971). *Palaeozoic Fishes*. Philadelphia,: Saunders.

Raffel, M., Willert, C. and Kompenhans, J. (1998). *Particle Image Velocimetry: A Practical Guide*. Heidelberg: Springer-Verlag.

Rome, L. C., Swank, D. and Corda, D. (1993). How fish power swimming. *Science* **261**, 340–343.

Rosen, D. E. (1982). Teleostean interrelationships, morphological function and evolutionary inference. *Am. Zool.* **22**, 261–273.

SAS Institute (1996). *SAS/STAT System for Personal Computers, Version 6.12*. Cary, NC: SAS Institute.

Schmidt, E. M. and Lauder, G. V. (1995). Kinematics of locomotion in sturgeon: do heterocercal tails function similarly? *Am. Zool.* **35**, 62A.

Scott, W. B. and Crossman, E. J. (1973). *Freshwater Fishes of Canada*. Ottawa: Fisheries Research Board of Canada.

Simons, J. R. (1970). The direction of the thrust produced by the heterocercal tails of two dissimilar elasmobranchs: the Port Jackson shark, *Heterodontus portusjacksoni* (Meyer) and the piked dogfish, *Squalus megalops* (Macleay). *J. Exp. Biol.* **52**, 95–107.

Simons, M. (1994). *Model Aircraft Aerodynamics*. Herts, UK: Argus Books.

Smith, H. C. (1992). *The Illustrated Guide to Aerodynamics*. New York: TAB Books.

Thomson, K. S. (1976). On the heterocercal tail in sharks. *Paleobiol.* **2**, 19–38.

Videler, J. J. (1993). *Fish Swimming*. New York: Chapman & Hall.

Vogel, S. (1994). *Life in Moving Fluids. The Physical Biology of Flow*. Second edition. Princeton: Princeton University Press.

Walker, J. A. and Westneat, M. W. (1997). Labriform propulsion in fishes: kinematics of flapping aquatic flight in the bird wrasse *Gomphosus varius* (Labridae). *J. Exp. Biol.* **200**, 1549–1569.

Webb, P. W. (1973). Kinematics of pectoral fin propulsion in *Cymatogaster aggregata*. *J. Exp. Biol.* **59**, 697–710.

Webb, P. W. (1986). Kinematics of lake sturgeon, *Acipenser fulvescens*, at cruising speeds. *Can. J. Zool.* **64**, 2137–2141.

Webb, P. W. (1993a). The effect of solid and porous channel walls

on steady swimming of steelhead trout *Oncorhynchus mykiss*. *J. Exp. Biol.* **178**, 97–108.

Webb, P. W. (1993b). Is tilting behavior at low swimming speeds unique to negatively buoyant fish? Observations on steelhead trout, *Oncorhynchus mykiss*, and bluegill, *Lepomis macrochirus*. *J. Fish Biol.* **43**, 687–694.

Webb, P. W. and Weihs, D. (1994). Hydrostatic stability of fish with swim bladders: not all fish are unstable. *Can. J. Zool.* **72**, 1149–1154.

Wegener, P. P. (1997). *What Makes Airplanes Fly?* New York: Springer.

Westneat, M. W. (1996). Functional morphology of aquatic flight in fishes: kinematics, electromyography and mechanical modeling of labriform locomotion. *Am. Zool.* **36**, 582–598.

Westneat, M. W. and Walker, J. A. (1997). Motor patterns of labriform locomotion: kinematic and electromyographic analysis of pectoral fin swimming in the labrid fish *Gomphosus varius*. *J. Exp. Biol.* **200**, 1881–1893.

Wilga, C. D. and Motta, P. J. (1998a). Conservation and variation in the feeding mechanism of the spiny dogfish *Squalus acanthias*. *J. Exp. Biol.* **201**, 1345–1358.

Wilga, C. D. and Motta, P. J. (1998b). Feeding mechanism of the Atlantic guitarfish *Rhinobatos lentiginosus*: modulation of kinematic and motor activity. *J. Exp. Biol.* **201**, 3167–3184.

Willert, C. E. and Gharib, M. (1991). Digital particle image velocimetry. *Experiments Fluids* **10**, 181–193.

Zar, J. H. (1996). *Biostatistical Analysis*. Upper Saddle River, NJ: Prentice Hall.